

A Three-Dimensional
Neutron Diffusion Calculation Code :
DIFFUSION-ACE

July 1979

日 本 原 子 力 研 究 所

Japan Atomic Energy Research Institute

JAERI レポート

この報告書は、日本原子力研究所で行なわれた研究および技術の成果を研究成果編集委員会の審査を経て、不定期に刊行しているものです。

研究成果編集委員会

委員長 野 沢 俊 弥 (理事)

委 員

赤石 準 (保健物理部)	田中 正俊 (核融合研究部)
朝岡 卓見 (原子炉工学部)	仲本秀四郎 (技術情報部)
伊藤 太郎 (企画室)	長崎 隆吉 (燃料工学部)
今井 和彦 (環境安全研究部)	橋谷 博 (原子炉化学部)
神原 忠則 (材料試験炉部)	浜口 由和 (物理部)
栗山 将 (高崎研究所)	原 昌雄 (動力炉開発・安全性研究管理部)
佐々木吉方 (研究炉管理部)	原田吉之助 (物理部)
佐藤 一男 (安全解析部)	松浦祥次郎 (動力試験炉部)
佐野川好母 (高温工学室)	三井 光 (高崎研究所)
四方 英治 (製造部)	森島 淳好 (安全工学部)
田川 博章 (原子炉化学部)	

入手 (資料交換による)、複製などのお問い合わせは、日本原子力研究所技術情報部 (〒319-11 茨城県那珂郡東海村) であて、お申し込みください。なお、このほかに財団法人原子力弘済会資料センター (茨城県那珂郡東海村日本原子力研究所内) で複写による実費頒布をおこなっております。

JAERI Report

Published by the Japan Atomic Energy Research Institute

Board of Editors

Toshiya Nozawa (Chief Editor)

Jun Akaishi	Kazuhiko Imai	Hiroshi Mitsui	Kazuo Sato
Takumi Asaoka	Taro Ito	Atuyoshi Morishima	Konomo Sanokawa
Yoshikazu Hamaguchi	Masanori Kanbara	Ryukichi Nagasaki	Eiji Shikata
Hiroshi Hashitani	Isamu Kuriyama	Hideshiro Nakamoto	Hiroaki Tagawa
Masao Hara	Shojiro Matsuura	Yoshikata Sasaki	Masatoshi Tanaka
Kichinosuke Harada			

Inquiries about the availability of reports and their reproduction should be addressed to the Division of Technical Information, Japan Atomic Energy Research Institute, Tokai-mura, Nakagun, Ibaraki-ken, Japan.

編集兼発行 日本原子力研究所
印刷 三美印刷株式会社

A Three-Dimensional Neutron Diffusion Calculation Code: DIFFUSION-ACE

Yoshitaka NAITO, Mitsuru MAEKAWA*, Kazuo SHIBUYA**

Division of JPDR

Received February 13, 1979

A computer code system named BWR-ACE has been developed for analysing the physical phenomena in a boiling water reactor (BWR). The BWR-ACE consists of three sub-systems, CROSS-ACE, STEADY-ACE and BURN-ACE. The sub-system STEADY-ACE which analyses the phenomena in a BWR under steady state consists of two programs, DIFFUSION-ACE and HYDRO-ACE. The program DIFFUSION-ACE described in this report is a routine to calculate the neutron flux distribution.

For calculating the neutron flux distribution in a reactor with a conventional fine-mesh difference approximation method, many mesh points and a long computer time are required. A new approximation method named "leakage iterative method" has been developed in order to obtain efficiently the neutron flux distribution in a light water moderated reactor by the difference approximation method. This method is embodied in the DIFFUSION-ACE program for the FACOM 230-75 and CDC-6600 computers. This report describes details of the method used in DIFFUSION-ACE and instructions to the user about input data requirements.

Keywords: Neutron Diffusion Code, Three-Dimensional Calculation, BWR, Leakage Iterative Method, Neutron Flux Distribution, Instruction Manual.

Present division

* General Electric Technical Services Co. Inc.

** FACOM Co. Inc.

3次元中性子拡散計算コード: DIFFUSION-ACE

内 藤 俣 孝, 前 川 充 留*, 渋谷 一 男**

東海研究所動力試験炉部

1979年2月13日 受理

沸騰水型動力炉 (BWR) 内の物理現象を解析するために計算コード・システム BWR-ACE を開発してきた。BWR-ACE は3つのサブシステム CROSS-ACE, STEADY-ACE および BURN-ACE よりなっている。定常状態における BWR 内の現象を解析するためのサブシステム STEADY-ACE は、2つのプログラム DIFFUSION-ACE と HYDRO-ACE よりなっている。このレポートで記す DIFFUSION-ACE は中性子束分布を計算するルーチンである。

従来の微細階差法で原子炉内の中性子束分布を計算するためには、多くのメッシュ点や長い計算時間が必要である。そこで、階差近似で軽水炉中の中性子束分布を効率的に求めるために、1つの新しい近似法“洩れ量繰返し法”を開発した。この手法を用いて計算機 FACOM 230-75 および CDC-6600 用のプログラム DIFFUSION-ACE を開発した。

本報告書には、プログラム DIFFUSION-ACE の中で使用されている計算手法の詳細と使用者が用意すべき入力データについて記す。

現在の所属

* ジェネラル・エレクトリック・テクニカル・サービス株式会社

** 富士通株式会社

Contents

1. Introduction	1
2. Theory	2
2.1 Outline of leakage iterative method.....	2
2.2 Fundamental equation	3
2.3 Convergence condition of the method.....	5
2.4 Initial guess of neutron source	11
2.5 Calculation of neutron flux in reflector	13
3. Test Calculations.....	21
4. Guide to User	24
4.1 Overall program flow	24
4.2 Discretization of spatial variables	24
4.3 Description of input data	27
4.4 Output description	33
4.5 Sample problem.....	33
5. Conclusions	34
Acknowledgement	34
References.....	34
Appendix A Input Data of Sample Problem	35
Appendix B Output Data of Sample Problem	37

目 次

1. 序 論.....	1
2. 理 論.....	2
2.1 もれ量繰返し法の概要	2
2.2 基礎方程式	3
2.3 収束条件	5
2.4 中性子源の初期推定値	11
2.5 反射体内の中性子束の計算	13
3. テスト計算.....	21
4. 使用者に対する手引き.....	24
4.1 プログラムの全体の流れ	24
4.2 空間分割	24
4.3 入力データ・フォーマット	27
4.4 出 力 量	33
4.5 例 題	33
5. 結 論.....	34
謝 辞.....	34
参考文献.....	34
付 録	
A 例題の入力データ	35
B 例題の出力データ	37

1. Introduction

Various methods have been proposed for solving a three-dimensional neutron diffusion equation. The most straightforward and reliable method is based on the fine-mesh difference approximation combined with the iterative solution technique. The method, however, is not always practical for design calculations of large nuclear power reactors because the required computation time and memory are enormous. Many other approximation methods have been developed to reduce the computation time, which include the flux synthesis method and the coarse-mesh finite-difference approximation method. The most famous synthesis method uses either variational flux synthesis or multichannel flux synthesis¹⁾. The solution by the flux synthesis method is obtained in a form different from that by the fine-mesh difference approximation, so it is not easy to compare the calculational results and to make the error analysis²⁾. In addition, the condition of convergence of the multichannel flux synthesis method is not clear. The disadvantage of the coarse-mesh finite difference approximation is that the discretization error in the calculation of neutron leakage from a subregion is generally large because the mesh widths are larger than the diffusion length.

To eliminate the drawbacks of these methods, a "leakage iterative method" is proposed in this paper. This method is embodied in the DIFFUSION-ACE program in the computer code system BWR-ACE designed for analysing the physical phenomena in a boiling water reactor (BWR) on the FACOM 230-75 and CDC-6600 computers. The BWR-ACE consists of three sub-systems, CROSS-ACE, STEADY-ACE and BURN-ACE. The sub-system STEADY-ACE which analyses the phenomena in a BWR under steady state, consists of two programs DIFFUSION-ACE and HYDRO-ACE. The program DIFFUSION-ACE calculates the thermal power distribution and the program HYDRO-ACE deals with the thermal hydraulics in a BWR. In this sub-system STEADY-ACE, the two programs DIFFUSION-ACE and HYDRO-ACE are used iteratively until the thermal power distribution and the coolant void distribution become consistent with each other.

This report presents details of the method used in DIFFUSION-ACE program for solving speedily three-dimensional neutron diffusion equation and instructions to user about input data requirements.

2. Theory

2.1 Outline of leakage iterative method

The reactor is divided into several layers along the z axis and into several rectangular channels perpendicular to the xy plane as shown in Fig. 1. A parallelepiped formed by a channel and a layer is called a block in which the materials are homogenized. To start the iterative procedure for solving the diffusion equation, the neutron source and the radial leakage coefficients are arbitrarily assumed initially as shown in Fig. 2. A one-dimensional neutron flux calculation is performed for each channel with the radial leakage coefficient. A two-dimensional neutron flux calculation is then made for each layer with the axial leakage determined from the one-dimensional calculation. The one- and two-dimensional leakage will be iterated until the consistency is attained between the two. At each step of the iteration the neutron source distribution and the eigenvalue are recalculated. For obtaining the balance of the neutron population within a block, it is important to evaluate the neutron leakage from the block as precisely as possible. For this purpose, a block is subdivided into fine meshes, and the fine-mesh difference approximation method is applied to solve the one- and two-dimensional neutron diffusion equations for each channel and layer, respectively.

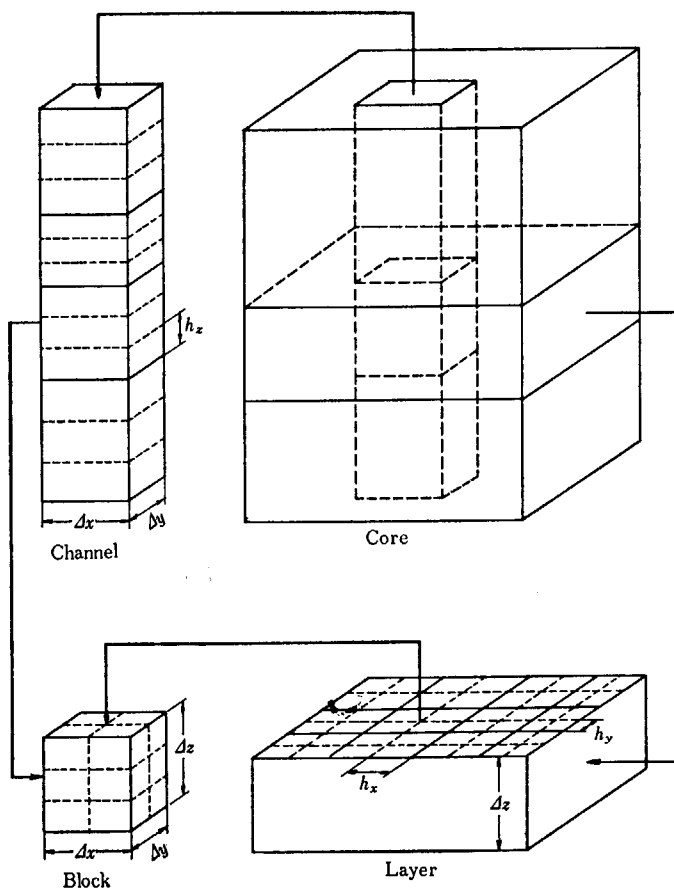


Fig. 1 Configuration of channels, layers and blocks.

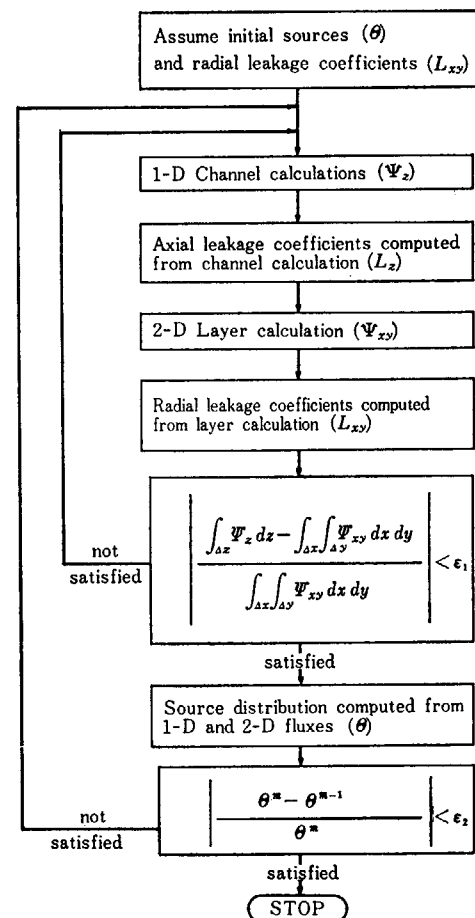


Fig. 2 Schematic diagram of the leakage iterative method.

The present method has the following characteristics :

1) A fine-mesh difference approximation technique is applied only to the channels and layers. Therefore it is not necessary to calculate the neutron fluxes at all fine-mesh points in the core and thus the computer time is reduced. If the block is a 12cm cube and the mesh width is 2 cm, the number of fine-mesh points is $6 \times 6 \times 6 = 216$. In the present method, however, the number of mesh points is $6 + (6 \times 6) = 42$, that is about one-fifth of the former. The terms connecting the channel and layer calculations are only the neutron leakage and the neutron source, which reduce the computer memory required.

2) Since the neutron leakage from a block is calculated by a fine-mesh difference approximation, the discretization error is minimized.

3) When only one fine-mesh point is located in each block, this method becomes the same as a fine-mesh difference approximation. In this case, the iterative scheme corresponds to one of the variants of the Peaceman-Rachford iterative method. Therefore, it is possible to establish the condition under which the consistency is achieved between the axial and radial leakages in the same manner as ADI (alternating direction implicit iterative method due to Peaceman and Rachford), and it is easy to compare the results with those obtained from conventional fine-mesh difference approximation methods. The computer code can be used for calculating both the collapsed flux and the fine-mesh flux.

2.2 Fundamental equation

The iterative process to recalculate the source distribution with the previously obtained neutron flux is the same as that utilized in the conventional power-iteration method. This iterative process is called as the outer iteration or source iteration, and the convergence condition has been shown by many workers.

The problem with which we are concerned here is how to calculate the neutron flux distribution for a fixed neutron source distribution. This process is called as the inner iteration. The important points to be noted concerning the convergence of the inner iteration are :

- 1) the equation is for a volume-integrated flux
- 2) the calculation is repeated along the channels and layers alternately
- 3) the axial and radial leakages are contained in the diagonal elements of the operator matrix, so that the elements are recalculated at each iteration step.

The fundamental equation to be solved is

$$\nabla D \nabla \phi - \Sigma_T \phi + \theta = 0, \quad (1)$$

where ϕ is the neutron flux and θ the neutron source at a fine-mesh point, and D and Σ_T are the diffusion coefficient and the macroscopic total cross section, respectively, for a homogenized block.

Integrating Eq. (1) over a block results in

$$\begin{aligned} D \int_{\Delta x} \int_{\Delta y} dx dy \int_{\Delta z} \frac{\partial^2 \phi}{\partial z^2} dz + D \int_{\Delta z} dz \int_{\Delta x} \int_{\Delta y} \left(\frac{\partial^2}{\partial x^2} + \frac{\partial^2}{\partial y^2} \right) \phi dx dy \\ - \Sigma_T \int_{\Delta x} \int_{\Delta y} \int_{\Delta z} \phi dx dy dz + \int_{\Delta x} \int_{\Delta y} \int_{\Delta z} \theta dx dy dz = 0, \end{aligned} \quad (2)$$

where Δx , Δy , and Δz are the widths of the homogenized block. Using the following notations :

$$-l_z \equiv \frac{\int_{\Delta x} \int_{\Delta y} dx dy \int_{\Delta z} D \frac{\partial^2 \phi}{\partial z^2} dz}{\int_{\Delta x} \int_{\Delta y} \int_{\Delta z} \phi dx dy dz},$$

$$\begin{aligned}
-l_{xy} &\equiv \frac{\int_{dz} dz \int_{dx} \int_{dy} D \left(\frac{\partial^2}{\partial x^2} + \frac{\partial^2}{\partial y^2} \right) \phi dx dy}{\int_{dx} \int_{dy} \int_{dz} \phi dx dy dz}, \\
\phi_z &\equiv \int_{dx} \int_{dy} \phi dx dy, \quad \phi_{xy} \equiv \int_{dz} \phi dz, \\
\theta_z &\equiv \int_{dx} \int_{dy} \theta dx dy, \quad \theta_{xy} \equiv \int_{dz} \theta dz,
\end{aligned} \tag{3}$$

Equation (2) is rewritten as

$$\int_{dz} D \frac{\partial^2 \phi_z}{\partial z^2} dz - \int_{dz} (\Sigma_T + l_{xy}) \phi_z dz + \int_{dz} \theta_z dz = 0, \tag{4}$$

$$\int_{dx} \int_{dy} D \left(\frac{\partial^2}{\partial x^2} + \frac{\partial^2}{\partial y^2} \right) \phi_{xy} dx dy - \int_{dx} \int_{dy} (\Sigma_T + l_z) \phi_{xy} dx dy + \int_{dx} \int_{dy} \theta_{xy} dx dy = 0, \tag{5}$$

where ϕ_z and ϕ_{xy} are obtained respectively by solving the following one- and two-dimensional fine-mesh neutron diffusion equations:

$$D \frac{\partial^2 \phi_z}{\partial z^2} - (\Sigma_T + l_{xy}) \phi_z + \theta_z = 0, \tag{6}$$

$$D \left(\frac{\partial^2}{\partial x^2} + \frac{\partial^2}{\partial y^2} \right) \phi_{xy} - (\Sigma_T + l_z) \phi_{xy} + \theta_{xy} = 0. \tag{7}$$

One-dimensional fine-mesh neutron flux distribution calculations are performed along the channels, and two-dimensional calculations are made in the layers. The axial and radial leakages from each block, l_z and l_{xy} , are obtained as follows:

$$\begin{aligned}
-l_z &= \frac{\int_{dz} D \frac{\partial^2 \phi_z}{\partial z^2} dz}{\int_{dz} \phi_z dz}, \\
-l_{xy} &= \frac{\int_{dx} \int_{dy} D \left(\frac{\partial^2}{\partial x^2} + \frac{\partial^2}{\partial y^2} \right) \phi_{xy} dx dy}{\int_{dx} \int_{dy} \phi_{xy} dx dy}.
\end{aligned} \tag{8}$$

The neutron flux distribution in the core is determined by solving Eqs. (6) and (7) alternately.

The neutron flux convergence criterion is given by

$$\left| \frac{\int_{dz} \phi_z dz - \int_{dx} \int_{dy} \phi_{xy} dx dy}{\int_{dz} \phi_z dz} \right| < E. \tag{9}$$

If the neutron flux distribution satisfies the above condition, the leakage coefficients also satisfy the following condition, as is readily seen from Eqs. (4), (5) and (8):

$$\begin{aligned}
&|l_{xy}^{\text{new}} - l_{xy}^{\text{old}}| \\
&= \frac{\int_{dx} \int_{dy} \theta_{xy} dx dy}{\int_{dx} \int_{dy} \phi_{xy} dx dy} \cdot \left| \frac{\int_{dz} \phi_z dz - \int_{dx} \int_{dy} \phi_{xy} dx dy}{\int_{dz} \phi_z dz} \right| < \frac{\int_{dx} \int_{dy} \theta_{xy} dx dy}{\int_{dx} \int_{dy} \phi_{xy} dx dy} \cdot E.
\end{aligned} \tag{10}$$

The suffix *new* indicates the result of this iteration step and *old* the result of the preceding iteration step.

After the neutron flux convergence criterion is satisfied, the neutron sources, θ_{xy} and θ_z , are recalculated by using the converged neutron fluxes ϕ_z and ϕ_{xy} . The source iteration process is repeated until the source distribution is covered.

2.3 Convergence condition of the method

We discuss here the conditions under which the iterative scheme of the leakage iterative method converges, by expressing Eqs. (4) and (5) in finite difference forms. The set of one-dimensional equations along channels is written as

$$A_z \vec{\phi}_z = \vec{\Theta}_z, \quad (11)$$

where $\vec{\Theta}_z$ is the neutron source vector. The operator matrix A_z for fine-mesh points is subdivided into

$$A_z \equiv (D_z - B_z) + \Sigma_z + \tilde{L}_{xy}, \quad (12)$$

where the matrices $(D_z - B_z)$ and Σ_z are the diffusion and removal operator matrices, respectively. The matrix D_z is diagonal and $(D_z - B_z) + \Sigma_z$ is tridiagonal which has the following characteristics; (a) irreducible, (b) symmetric, (c) diagonally dominant, and (d) positive definite. The radial leakage coefficient matrix \tilde{L}_{xy} is a diagonal matrix, whose elements consist of l_{xy} .

The set of two-dimensional equations in the layers can similarly be expressed as follows:

$$A_{xy} \vec{\phi}_{xy} = \vec{\Theta}_{xy}, \quad (13)$$

where

$$A_{xy} = (D_{xy} - B_{xy}) + \Sigma_{xy} + \tilde{L}_z. \quad (14)$$

In Eq. (14), the matrix $(D_{xy} - B_{xy}) + \Sigma_{xy}$ has the same characteristics as $(D_z - B_z) + \Sigma_z$, and \tilde{L}_z denotes the axial leakage coefficient matrix.

To express the dimension of these matrices, the following notations are used:

N_{ch} = number of channels

N_{fz} = number of one-dimensional fine-mesh points per channel

N_{fzt} = total number of one-dimensional fine-mesh points in the core, which is equal to $N_{fz} \cdot$

N_{ch}

N_{lay} = number of layers

N_{fxy} = number of two-dimensional fine-mesh points per layer

N_{fxyt} = total number of two-dimensional fine-mesh points in the core, which is equal to $N_{fxy} \cdot$

N_{lay}

N_b = number of blocks which is equal to $N_{ch} \cdot N_{lay}$.

Now we introduce a summation matrix, S , and an expansion matrix, R . By operating the summation matrix, quantities such as the flux and the leakage coefficient are integrated over a block. By operating the expansion matrix, on the other hand, the block leakage coefficient matrix, (N_b, N_b) , becomes (N_{fzt}, N_{fzt}) or (N_{fxyt}, N_{fxyt}) . The matrices S and R satisfy the following relations:

$$S_z R_z = I, \quad S_{xy} R_{xy} = I, \quad (15)$$

where I is a unit matrix.

To make it easy to understand the relations between matrices and vectors, the mesh specification and the matrix form are shown in Figs. 3 and 4. Some examples of the summation matrices and the expansion matrices are shown in Figs. 5 and 6, respectively. As shown in these examples, the neutron flux integrated over a block is expressed as $S_z \vec{\phi}_z$ or $S_{xy} \vec{\phi}_{xy}$, and the value of $S_z \vec{\phi}_z$ is equal to that of $S_{xy} \vec{\phi}_{xy}$. The axial and radial leakages from a block are expressed as $S_z(D_z - B_z) \vec{\phi}_z$ and $S_{xy}(D_{xy} - B_{xy}) \vec{\phi}_{xy}$, respectively.

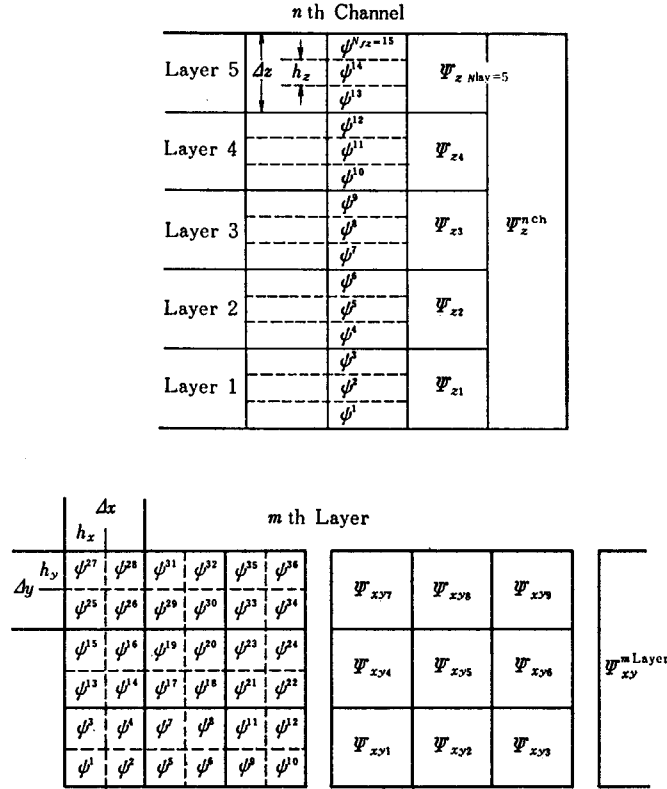
Equations (4), (5), and (8) can be rewritten in matrix forms as

$$S_z(D_z - B_z) \vec{\phi}_z + S_z(\Sigma_z + \tilde{L}_{xy}) \vec{\phi}_z = S_z \vec{\Theta}_z, \quad (16)$$

$$S_{xy}(D_{xy}-B_{xy})\vec{\phi}_{xy}+S_{xy}(\Sigma_{xy}+\tilde{L}_z)\vec{\phi}_{xy}=S_{xy}\vec{\Theta}_{xy} , \quad (17)$$

$$L_z S_z \vec{\phi}_z = S_z (D_z - B_z) \vec{\phi}_z ,$$

$$L_{xy} S_{xy} \vec{\phi}_{xy} = S_{xy} (D_{xy} - B_{xy}) \vec{\phi}_{xy} . \quad (18)$$



$$N_{ch}=9, N_{lay}=5, N_{fz}=3 \times 5=15, N_{fxy}=4 \times 9=36$$

$$N_{fzt}=N_{fz} \times N_{ch}=135, N_{fxyt}=N_{fxy} \times N_{lay}=180$$

Fig. 3 Schematic representation of the collapsed fluxes.

The dimensions of the summation matrices S_z and S_{xy} are (N_b, N_{fzt}) and (N_b, N_{fxyt}) , respectively, and the dimensions of the fine leakage matrices \tilde{L}_{xy} and \tilde{L}_z are (N_{fzt}, N_{fzt}) and (N_{fxyt}, N_{fxyt}) , respectively. The block leakage matrices L_{xy} and L_z are (N_b, N_b) matrices. The matrix \tilde{L}_{xy} is expressed by L_{xy} as

$$\tilde{L}_{xy} = R_z L_{xy} S_z \quad (19)$$

and, similarly,

$$\tilde{L}_z = R_{xy} L_z S_{xy} , \quad (20)$$

where the expansion matrices, R_z and R_{xy} , are (N_{fzt}, N_b) and (N_{fxyt}, N_b) , respectively. The matrices \tilde{L}_z and \tilde{L}_{xy} belong to the fine-mesh points, while L_z and L_{xy} belong to the blocks and operate on the integrated flux over a block. Using these expressions, the iteration scheme is written as

$$\begin{aligned} & (D_z - B_z) \vec{\phi}_z^m + \Sigma_z \vec{\phi}_z^m + \gamma R_z L_{xy}^{m-1} S_z \vec{\phi}_z^m \\ & = (\gamma - 1) R_z S_{xy} (D_{xy} - B_{xy}) \vec{\phi}_{xy}^{m-1} + \vec{\Theta}_z , \end{aligned} \quad (21)$$

$$\begin{aligned} & (D_{xy} - B_{xy}) \vec{\phi}_{xy}^{m+1} + \Sigma_{xy} \vec{\phi}_{xy}^{m+1} + \gamma' R_{xy} L_z^m S_{xy} \vec{\phi}_{xy}^{m+1} \\ & = (\gamma' - 1) R_{xy} S_z (D_z - B_z) \vec{\phi}_z^m + \vec{\Theta}_{xy} . \end{aligned} \quad (22)$$

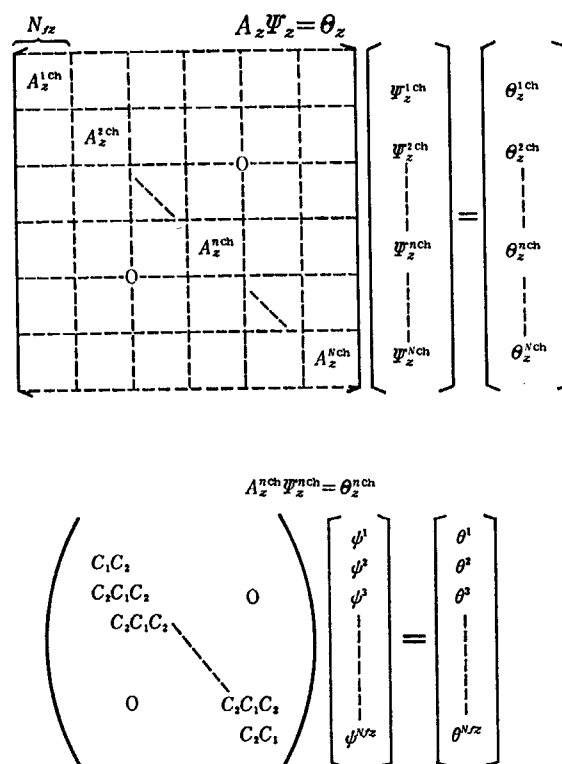


Fig. 4 Schematic representation of the relationship between operator matrices and vectors.

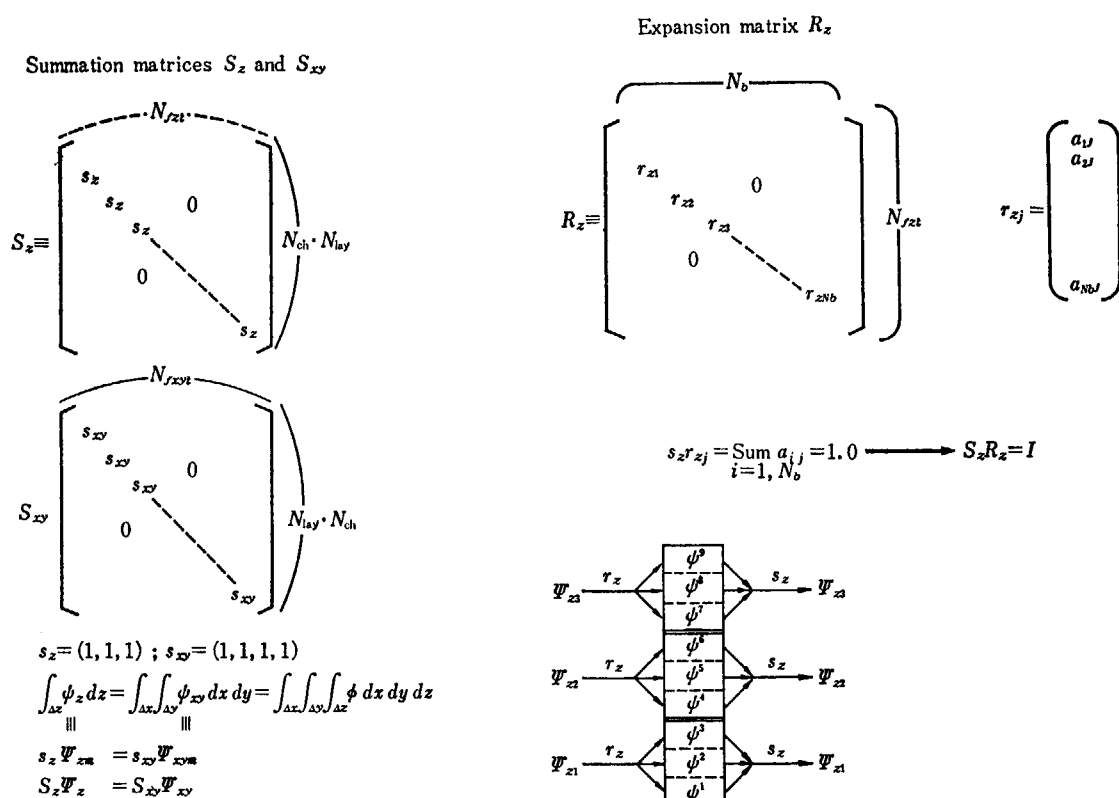


Fig. 5 Schematic representation of the summation matrices.

Fig. 6 Schematic representation of the expansion matrix.

In the above expressions, m and $m+1$ stand for the iteration steps, and γ and γ' are acceleration parameters. Using the relations of Eqs. (19) and (20), the vectors of Eqs. (11) and (13) are expressed as follows:

$$(D_z - B_z)\vec{\phi}_z + \Sigma_z \vec{\phi}_z + R_z S_{xy}(D_{xy} - B_{xy})\vec{\phi}_{xy} = \Theta_z, \quad (23)$$

$$(D_{xy} - B_{xy})\vec{\phi}_{xy} + \Sigma_{xy} \vec{\phi}_{xy} + R_{xy} S_z(D_z - B_z)\vec{\phi}_z = \Theta_{xy}. \quad (24)$$

Subtracting Eq. (21) from (23), we get

$$\begin{aligned} & [(D_z - B_z) + \Sigma_z](\vec{\phi}_z - \vec{\phi}_z^m) + R_z S_{xy}(D_{xy} - B_{xy})(\vec{\phi}_{xy} - \vec{\phi}_{xy}^{m-1}) \\ &= \gamma[R_z L_{xy}^{m-1} S_z \vec{\phi}_z^m - R_z S_{xy}(D_{xy} - B_{xy})\vec{\phi}_{xy}^{m-1}] \\ &= \gamma R_z L_{xy}^{m-1} [S_z \vec{\phi}_z^m - S_{xy} \vec{\phi}_{xy}^{m-1}] \\ &= \gamma R_z L_{xy}^{m-1} S_z (\vec{\phi}_z^m - \vec{\phi}_z) + \gamma R_z L_{xy}^{m-1} S_{xy} (\vec{\phi}_{xy} - \vec{\phi}_{xy}^{m-1}). \end{aligned} \quad (25)$$

Defining the error vector as

$$\vec{E}_z^m \equiv \vec{\phi}_z - \vec{\phi}_z^m, \quad \vec{E}_{xy}^{m-1} \equiv \vec{\phi}_{xy} - \vec{\phi}_{xy}^{m-1}, \quad (26)$$

Eq. (25) is expressed as

$$\begin{aligned} & [(D_z - B_z) + \Sigma_z + \gamma R_z L_{xy}^{m-1} S_z] \vec{E}_z^m \\ &= [\gamma R_z L_{xy}^{m-1} S_{xy} - R_z S_{xy}(D_{xy} - B_{xy})] \vec{E}_{xy}^{m-1}. \end{aligned} \quad (27)$$

In the same way, from Eqs. (22) and (24),

$$\begin{aligned} & [(D_{xy} - B_{xy}) + \Sigma_{xy} + \gamma' R_{xy} L_z^m S_{xy}] \vec{E}_{xy}^{m+1} \\ &= [\gamma' R_{xy} L_z^m S_z - R_{xy} S_z(D_z - B_z)] \vec{E}_z^m. \end{aligned} \quad (28)$$

Equations (27) and (28) give

$$\begin{aligned} \vec{E}_{xy}^{m+1} &= [(D_{xy} - B_{xy}) + \Sigma_{xy} + \gamma' R_{xy} L_z^m S_{xy}]^{-1} \\ &\quad \times [\gamma' R_{xy} L_z^m S_z - R_{xy} S_z(D_z - B_z)] \\ &\quad \times [(D_z - B_z) + \Sigma_z + \gamma R_z L_{xy}^{m-1} S_z]^{-1} \\ &\quad \times [\gamma R_z L_{xy}^{m-1} S_{xy} - R_z S_{xy}(D_{xy} - B_{xy})] \vec{E}_{xy}^{m-1}. \end{aligned} \quad (29)$$

The matrices H_1 and H_2 are now defined as

$$\begin{aligned} H_1 &\equiv (D_z - B_z) + \frac{1}{2} \Sigma_z \\ H_2 &\equiv (D_{xy} - B_{xy}) + \frac{1}{2} \Sigma_{xy}. \end{aligned} \quad (30)$$

Using Eqs. (30) and (15), Eq. (29) can be rewritten as

$$\begin{aligned} \vec{E}_{xy}^{m+1} &= \left[\left(H_2 + \frac{1}{2} \Sigma_{xy} \right) + \gamma' R_{xy} L_z^m S_{xy} \right]^{-1} \\ &\quad \times R_{xy} S_z \left[\left(H_1 - \frac{1}{2} \Sigma_z \right) - \gamma' R_z L_z^m S_z \right] \\ &\quad \times \left[\left(H_1 - \frac{1}{2} \Sigma_z \right) + \gamma R_z L_{xy}^{m-1} S_z + \Sigma_z \right]^{-1} R_z S_{xy} \\ &\quad \times \left[\left(H_2 + \frac{1}{2} \Sigma_{xy} \right) - \gamma R_{xy} L_{xy}^{m-1} S_{xy} - \Sigma_{xy} \right] \vec{E}_{xy}^{m-1}. \end{aligned} \quad (31)$$

The four diagonal matrices, F , α , G and β , are defined as

$$\begin{aligned} F + \alpha &\equiv \gamma' R_z L_z^m S_z, \\ F - \alpha &\equiv \gamma R_z L_{xy}^{m-1} S_z + \Sigma_z, \\ G + \beta &\equiv \gamma' R_{xy} L_z^m S_{xy}, \\ G - \beta &\equiv \gamma R_{xy} L_{xy}^{m-1} S_{xy} + \Sigma_{xy}. \end{aligned} \quad (32)$$

These are rewritten in the form:

$$\begin{aligned} F &= \frac{1}{2} [\gamma' R_z L_z^m S_z + \gamma R_z L_{xy}^{m-1} S_z + \Sigma_z], \\ \alpha &= \frac{1}{2} [\gamma' R_z L_z^m S_z - \gamma R_z L_{xy}^{m-1} S_z - \Sigma_z], \end{aligned}$$

$$G = \frac{1}{2} [\gamma' R_{xy} L_z^m S_{xy} + \gamma R_{xy} L_{xy}^{m-1} S_{xy} + \Sigma_{xy}] ,$$

$$\beta = \frac{1}{2} [\gamma' R_{xy} L_z^m S_{xy} - \gamma R_{xy} L_{xy}^{m-1} S_{xy} - \Sigma_{xy}] . \quad (33)$$

Two matrices \tilde{H}_1 and \tilde{H}_2 are further defined as

$$\tilde{H}_1 \equiv H_1 - \frac{1}{2} \Sigma_z - \alpha ,$$

$$\tilde{H}_2 \equiv H_2 + \frac{1}{2} \Sigma_{xy} + \beta . \quad (34)$$

The error vector is thus given as

$$\vec{E}_{xy}^{m+1} = T \vec{E}_{xy}^{m-1} , \quad (35)$$

where

$$T \equiv (\tilde{H}_2 + G)^{-1} R_{xy} S_z (\tilde{H}_1 - F) (\tilde{H}_1 + F)^{-1} R_z S_{xy} (\tilde{H}_2 - G) . \quad (36)$$

A matrix \tilde{T} defined as

$$\tilde{T} \equiv (\tilde{H}_2 + G) T (\tilde{H}_2 + G)^{-1}$$

is similar to T and has the same eigenvalues as T . Using the relation of Eq. (36), we have

$$\tilde{T} = R_{xy} S_z (\tilde{H}_1 - F) (\tilde{H}_1 + F)^{-1} R_z S_{xy} (\tilde{H}_2 - G) (\tilde{H}_2 + G)^{-1} . \quad (37)$$

It is well known that the spectral radius of T , $\rho(T)$, is the same as that of \tilde{T} . The value is generally smaller than the matrix norm :

$$\begin{aligned} \rho(T) = \rho(\tilde{T}) &< \|\tilde{T}\| < \|R_{xy} S_z\| \\ &\times \|(\tilde{H}_1 - F)(\tilde{H}_1 + F)^{-1}\| \\ &\times \|R_z S_{xy}\| \cdot \|(\tilde{H}_2 - G)(\tilde{H}_2 + G)^{-1}\| . \end{aligned} \quad (38)$$

From the characteristics of summation and expansion matrices, the values of $\|R_{xy} S_z\|$ and $\|R_z S_{xy}\|$ can be chosen to satisfy the following relations :

$$\|R_{xy} S_z\| \leq \max_i [N_z(i)/N_{xy}(i)]$$

and

$$\|R_z S_{xy}\| \leq \max_i [N_{xy}(i)/N_z(i)] , \quad (39)$$

where $N_z(i)$, $N_{xy}(i)$ are the numbers of mesh points in the i -th block along the z axis and the xy plane, respectively. A proof of Eq. (39) is given in the following.

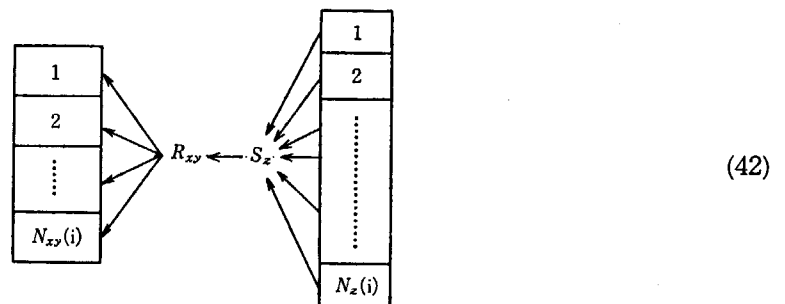
From the definition of a matrix norm :

$$\|R_{xy} S_z\| \equiv \sup_{\|\vec{x}\|=1} \|R_{xy} S_z \vec{x}\| , \quad (40)$$

the relation between vectors and matrices is expressed as

$$\vec{y} = R_{xy} S_z \vec{x} . \quad (41)$$

The above relation is expressed pictorially as



and in another form as

$$\begin{pmatrix} a_{11}[x_{11} + x_{12} + \dots + x_{1N_s(1)}] \\ a_{12}[x_{11} + x_{12} + \dots + x_{1N_s(1)}] \\ \vdots \\ a_{1N_{xy}(1)}[x_{11} + x_{12} + \dots + x_{1N_s(1)}] \\ a_{21}[x_{21} + x_{22} + \dots + x_{2N_s(2)}] \\ \vdots \\ a_{N_b N_{xy}(N_b)}[x_{N_b1} + x_{N_b2} + \dots + x_{N_b N_s(N_b)}] \end{pmatrix} = R_{xy} S_z \vec{x} . \quad (43)$$

From Eq. (43), the Euclidean norm of the vector is obtained directly :

$$\|R_{xy} S_z \vec{x}\| = \sum_{i=1, N_b} [a_{i1}^2 + a_{i2}^2 + \dots + a_{iN_{xy}(i)}^2] \times [x_{i1} + x_{i2} + \dots + x_{iN_s(i)}]^2 . \quad (44)$$

From the definition of a_{ij} , as shown Fig. 6,

$$a_{i1} + a_{i2} + \dots + a_{iN_{xy}(i)} = 1 . \quad (45)$$

If we consider the case of equal distribution, that is, $a_{ij} = a_{ik}$, the following relations are satisfied :

$$a_{ij} = 1/N_{xy}(i) \quad (46)$$

$$a_{i1}^2 + a_{i2}^2 + \dots + a_{iN_{xy}(i)}^2 = 1/N_{xy}(i) . \quad (47)$$

In this case, Eq. (40) becomes

$$\begin{aligned} \|R_{xy} S_z\| &\equiv \sup_{\|\vec{x}\|=1} \|R_{xy} S_z \vec{x}\| \\ &= \sup_{\|\vec{x}\|=1} \left\{ \sum_{i=1, N_b} \frac{1}{N_{xy}(i)} [x_{i1} + x_{i2} + \dots + x_{iN_s(i)}]^2 \right\} \\ &\leq \sup_{\|\vec{x}\|=1} \left\{ \sum_{i=1, N_b} \frac{N_z(i)}{N_{xy}(i)} [x_{i1}^2 + x_{i2}^2 + \dots + x_{iN_s(i)}^2] \right\} \\ &\leq \sup_{\|\vec{x}\|=1} \left\{ \max_i \left[\frac{N_z(i)}{N_{xy}(i)} \right] \cdot \sum_{i=1, N_b} [x_{i1}^2 + x_{i2}^2 + \dots + x_{iN_s(i)}^2] \right\} \\ &\leq \max_i \left[\frac{N_z(i)}{N_{xy}(i)} \right] . \end{aligned}$$

In the case of equal values of (N_z/N_{xy}) in every block in the core, the following relations is satisfied :

$$\|R_{xy} S_z\| \cdot \|R_z S_{xy}\| < 1 . \quad (48)$$

Since matrices F and G are diagonal and nonzero, matrices $F^{-1}\tilde{H}_1$ and $G^{-1}\tilde{H}_2$ are Hermitian and expressed as

$$\begin{aligned} F^{-1}\tilde{H}_1 &\equiv [\gamma' R_z L_z^m S_z + \gamma R_z L_{xy}^{m-1} S_z + \Sigma_z]^{-1} \\ &\quad \times \left[(D_z - B_z) + \frac{1}{2} (\Sigma_z - \gamma' R_z L_z^m S_z + \gamma R_z L_{xy}^{m-1} S_z) \right] , \\ G^{-1}\tilde{H}_2 &\equiv [\gamma R_{xy} L_z^m S_{xy} + \gamma R_{xy} L_{xy}^{m-1} S_{xy}]^{-1} \\ &\quad \times \left[(D_{xy} - B_{xy}) + \frac{1}{2} (\Sigma_{xy} - \gamma R_{xy} L_{xy}^{m-1} S_{xy} + \gamma' R_{xy} L_z^m S_{xy}) \right] . \end{aligned} \quad (49)$$

Assuming $F^{-1}\tilde{H}_1$ and $G^{-1}\tilde{H}_2$ to be positive definite, the following relations are satisfied :

$$\begin{aligned} \|(F^{-1}\tilde{H}_1 - I)(F^{-1}\tilde{H}_1 + I)^{-1}\| &= \max_{1 \leq j \leq n} \left| \frac{\lambda_j - 1}{\lambda_j + 1} \right| < 1 , \\ \|(G^{-1}\tilde{H}_2 - I)(G^{-1}\tilde{H}_2 + I)^{-1}\| &= \max_{1 \leq i \leq n} \left| \frac{\nu_i - 1}{\nu_i + 1} \right| < 1 . \end{aligned} \quad (50)$$

where λ_j and ν_i are the (positive) eigenvalues of the matrices $F^{-1}\tilde{H}_1$ and $G^{-1}\tilde{H}_2$, respectively³⁾.

If matrices $F^{-1}\tilde{H}_1$ and $G^{-1}\tilde{H}_2$ are positive definite, and summation and expansion matrices

are chosen to satisfy the condition (48), the spectral radius of the iteration matrix is less than unity :

$$\rho(T) < 1 . \quad (51)$$

This means that the error vectors E_{xy} and E_z converge to zero. If the proper values of γ and γ' are chosen, the matrices $F^{-1}\tilde{H}_1$ and $G^{-1}\tilde{H}_2$ become positive because the matrices $(D_z - B_z) + \frac{1}{2}\Sigma_z$ and $(D_{xy} - B_{xy}) + \frac{1}{2}\Sigma_{xy}$ are diagonally dominant.

When only one fine space mesh point is located in each block, this iterative scheme corresponds to a variant of the Peaceman-Rachford iterative method⁴⁾. In many cases, the acceleration parameters, γ and γ' , can be chosen to be unity, satisfying the above convergence conditions in the iterative scheme.

2.4 Initial guess of neutron source

In general, it is possible to reduce computation time by using a good guess of neutron source. The DIFFUSION-ACE has two options to obtain initial source guess. One is given from cards. The other is prepared in the computer code. In this case, radial leakage guess L_{xy} is required from the following theorem.

The fundamental diffusion equation (1) is integrated over Δx along x -coordinate, Δy along y -coordinate and $-\infty$ to $+\infty$ along z -coordinate :

$$\begin{aligned} & \int_{\Delta x} \int_{\Delta y} dx dy \int_{-\infty}^{\infty} D \left(\frac{\partial^2}{\partial x^2} + \frac{\partial^2}{\partial y^2} \right) \phi dz + \int_{\Delta x} \int_{\Delta y} dx dy \int_{-\infty}^{\infty} D \frac{\partial^2 \phi}{\partial z^2} dz \\ & - \int_{\Delta x} \int_{\Delta y} dx dy \int_{-\infty}^{\infty} \Sigma_T \phi dz + \int_{\Delta x} \int_{\Delta y} dx dy \int_{-\infty}^{\infty} S dz = 0 \end{aligned} \quad (52)$$

The following relation is assumed to be satisfied :

$$\int_{-\infty}^{\infty} D \frac{\partial^2 \phi}{\partial z^2} dz = 0 . \quad (53)$$

Following notations are now introduced :

$$\begin{aligned} \bar{\phi} & \equiv \int_{-\infty}^{\infty} \phi dz , \\ \bar{\theta} & \equiv \int_{-\infty}^{\infty} S dz , \\ \bar{D} & \equiv \frac{\int_{\Delta x} \int_{\Delta y} dx dy \int_{-\infty}^{\infty} D \left(\frac{\partial^2}{\partial x^2} + \frac{\partial^2}{\partial y^2} \right) \phi dz}{\int_{\Delta x} \int_{\Delta y} dx dy \int_{-\infty}^{\infty} \left(\frac{\partial^2}{\partial x^2} + \frac{\partial^2}{\partial y^2} \right) \phi dz} , \\ \bar{\Sigma}_T & \equiv \frac{\int_{\Delta x} \int_{\Delta y} dx dy \int_{-\infty}^{\infty} \Sigma_T \phi dz}{\int_{\Delta x} \int_{\Delta y} dx dy \int_{-\infty}^{\infty} \phi dz} . \end{aligned} \quad (54)$$

Equations (53) and (54) are substituted into Eq. (52) :

$$\bar{D} \int_{\Delta x} \int_{\Delta y} \left(\frac{\partial^2}{\partial x^2} + \frac{\partial^2}{\partial y^2} \right) \bar{\phi} dx dy - \bar{\Sigma}_T \int_{\Delta x} \int_{\Delta y} \bar{\phi} dx dy + \int_{\Delta x} \int_{\Delta y} \bar{\theta} dx dy = 0 . \quad (55)$$

Hence,

$$\bar{D} \left(\frac{\partial^2}{\partial x^2} + \frac{\partial^2}{\partial y^2} \right) \bar{\phi} - \bar{\Sigma}_T \bar{\phi} + \bar{\theta} = 0 . \quad (56)$$

In Eq. (56), for given \bar{D} and $\bar{\Sigma}_T$, the integrated flux $\bar{\phi}$ and source $\bar{\theta}$ are obtained by an iterative method. The $\bar{\theta}$ in an energy group g is given as follows :

$$\bar{\Theta}_g = \int_{-\infty}^{\infty} S^g dz = \frac{\chi^g}{\lambda} \text{Sum}_{g'} (\nu \bar{\Sigma}_t)^{g'g} \bar{\phi}^{g'} + \bar{\Sigma}_r^{g-1} \bar{\phi}^{g-1} \quad (57)$$

where

$$\begin{aligned} \nu \bar{\Sigma}_t^g &= \frac{\int_{\Delta x} \int_{\Delta y} dx dy \int_{-\infty}^{\infty} (\nu \Sigma_t)^g \phi^g dz}{\int_{\Delta x} \int_{\Delta y} dx dy \int_{-\infty}^{\infty} \phi^g dz}, \\ \bar{\Sigma}_r^g &= \frac{\int_{\Delta x} \int_{\Delta y} dx dy \int_{-\infty}^{\infty} (\nu \Sigma_r)^g \phi^g dz}{\int_{\Delta x} \int_{\Delta y} dx dy \int_{-\infty}^{\infty} \phi^g dz}. \end{aligned}$$

The initial source guess is obtained in the following manner. The one-dimensional neutron diffusion equation is solved using Eq. (6), and then ϕ_z and Θ_z are obtained. In this calculation, guess values of radial leakage l_{xy} are required. Using the above ϕ_z and Θ_z , integrated diffusion parameters are obtained as follows:

$$\begin{aligned} \bar{D} &= \frac{\int_{\Delta x} \int_{\Delta y} dx dy \int_{-\infty}^{\infty} D \left(\frac{\partial^2}{\partial x^2} + \frac{\partial^2}{\partial y^2} \right) \phi dz}{\int_{\Delta x} \int_{\Delta y} dx dy \int_{-\infty}^{\infty} \left(\frac{\partial^2}{\partial x^2} + \frac{\partial^2}{\partial y^2} \right) \phi dz} = \frac{\int_{-\infty}^{\infty} D l_{xy} \phi_z dz}{\int_{-\infty}^{\infty} l_{xy} \phi_z dz} \\ \bar{\Sigma}_T &= \frac{\int_{-\infty}^{\infty} \Sigma_T \phi_z dz}{\int_{-\infty}^{\infty} \phi_z dz}, \\ \nu \bar{\Sigma}_t &= \frac{\int_{-\infty}^{\infty} \nu \Sigma_t \phi_z dz}{\int_{-\infty}^{\infty} \phi_z dz}, \\ \bar{\Sigma}_r &= \frac{\int_{-\infty}^{\infty} \Sigma_r \phi_z dz}{\int_{-\infty}^{\infty} \phi_z dz}. \end{aligned} \quad (58)$$

The Θ_z is normalized as

$$\begin{aligned} \Theta_z^N &\equiv \frac{\Theta_z}{\int_{-\infty}^{\infty} \Theta_z dz} = \frac{\int_{\Delta x} \int_{\Delta y} S dx dy}{\int_{-\infty}^{\infty} dz \int_{\Delta x} \int_{\Delta y} S dx dy}, \\ \Theta_z^A &\equiv \frac{\int_{\Delta z} \Theta_z dz}{\int_{-\infty}^{\infty} \Theta_z dz} = \frac{\int_{\Delta x} \int_{\Delta y} \int_{\Delta z} S dx dy dz}{\int_{-\infty}^{\infty} dz \int_{\Delta x} \int_{\Delta y} S dx dy dz}. \end{aligned} \quad (59)$$

Equations (56) and (57) are now solved with Eq. (58). If the initial guess values of l_{xy} are correct, the eigenvalue λ obtained is the same as that from the three-dimensional calculation.

Using the results obtained by Eq. (56), the neutron source is normalized as follows:

$$\begin{aligned} \bar{\Theta}_{xy}^N &\equiv \frac{\bar{\Theta}}{\int_{-\infty}^{\infty} \int_{-\infty}^{\infty} \bar{\Theta} dx dy} = \frac{\int_{-\infty}^{\infty} S dz}{\int_{-\infty}^{\infty} \int_{-\infty}^{\infty} \int_{-\infty}^{\infty} S dx dy dz}, \\ \bar{\Theta}_{xy}^A &\equiv \frac{\int_{\Delta x} \int_{\Delta y} \bar{\Theta} dx dy}{\int_{-\infty}^{\infty} \int_{-\infty}^{\infty} \bar{\Theta} dx dy} = \frac{\int_{-\infty}^{\infty} dz \int_{\Delta x} \int_{\Delta y} S dx dy}{\int_{-\infty}^{\infty} \int_{-\infty}^{\infty} \int_{-\infty}^{\infty} S dx dy dz}. \end{aligned} \quad (60)$$

From Eqs. (59) and (60), initial source guess values for one- and two-dimensional calculations are expressed as follows :

$$\theta_z^{\text{guess}} = \frac{\int_{-\infty}^{\infty} \int_{-\infty}^{\infty} S dx dy}{\int_{-\infty}^{\infty} \int_{-\infty}^{\infty} \int_{-\infty}^{\infty} S dx dy dz} = \theta_z^N \cdot \bar{\theta}_{xy}^A, \quad (61)$$

$$\theta_{xy}^{\text{guess}} = \frac{\int_{-\infty}^{\infty} S dz}{\int_{-\infty}^{\infty} \int_{-\infty}^{\infty} \int_{-\infty}^{\infty} S dx dy dz} = \theta_z^A \cdot \bar{\theta}_{xy}^{-N} \quad (62)$$

If the initial guess of l_{xy} used in Eq. (6) is correct, the neutron source θ_z^{guess} and $\theta_{xy}^{\text{guess}}$ will be in agreement with the solution of three-dimensional diffusion equation, so that the more correct the initial guess of l_{xy} yields the better initial source guess and hence the computation time becomes shorter.

2.5 Calculation of neutron flux in reflector

For the analyses of a light water reactor by solving the neutron diffusion equation, a large number of mesh points are required because of the thermal neutron flux having a peak in the reflector. In some cases of three-dimensional calculations, more than half of mesh points are located in the reflector and therefore very large computer core memory and computer time are required. To diminish the mesh points in the reflector, the neutron flux in the core is calculated by the finite difference method while in the reflector it is calculated analytically. The flux distributions in the core and in the reflector are combined with boundary conditions to be satisfied.

First of all, this technique is explained on three-energy-group and one-dimensional neutron diffusion equations which are expressed as follows :

$$\left. \begin{aligned} \frac{d^2}{dl^2} \phi_R^1 - K_1^2 \phi_R^1 &= 0, & \text{for first group,} \\ \frac{d^2}{dl^2} \phi_R^2 - K_2^2 \phi_R^2 + \lambda_1 \phi_R^2 &= 0, & \text{for 2nd group,} \\ \frac{d^2}{dl^2} \phi_R^3 - K_3^2 \phi_R^3 + \lambda_2 \phi_R^3 &= 0, & \text{for 3rd group,} \end{aligned} \right\} \quad (63)$$

where

$$\begin{aligned} K_1^2 &= (\Sigma_{aR}^1 + \Sigma_{rR}^{1 \rightarrow 2} + D_R^1 B_R^1) / D_R^1, \\ K_2^2 &= (\Sigma_{aR}^2 + \Sigma_{rR}^{2 \rightarrow 3} + D_R^2 B_R^2) / D_R^2, \\ K_3^2 &= (\Sigma_{aR}^3 + D_R^3 B_R^3) / D_R^3, \\ \lambda_1 &= \Sigma_{rR}^{1 \rightarrow 2} / D_R^2, \\ \lambda_2 &= \Sigma_{rR}^{2 \rightarrow 3} / D_R^3, \end{aligned}$$

and B_R^g is the square of buckling at g -th energy-group in the reflector. At the above expression, the suffix R means reflector.

Equation (63) is solved under the following boundary conditions :

for $l=0$, $\phi_R^1 = \phi_B^1$, $\phi_R^2 = \phi_B^2$, $\phi_R^3 = \phi_B^3$, and for $l \rightarrow \infty$, $\phi_R^1 = \phi_R^2 = \phi_R^3 = 0$, where ϕ_R is a neutron flux in reflector and ϕ_B is a boundary neutron flux in core.

The solutions of Eq. (63) are

$$\left. \begin{aligned} \phi_R^1 &= A e^{-K_1 l}, \\ \phi_R^2 &= B e^{-K_2 l} + C e^{-\lambda_1 l}, \\ \phi_R^3 &= D e^{-K_3 l} + E e^{-\lambda_2 l} + F e^{-\lambda_3 l} \end{aligned} \right\} \quad (64)$$

where coefficients A , B , C , D , E and F are obtained by the boundary conditions as follows :

$$\left. \begin{aligned} A &= \phi_B^1, \\ B &= \phi_B^2 - \frac{\lambda_1}{K_2^2 - K_1^2} \phi_B^1, \\ C &= \frac{\lambda_1}{K_2^2 - K_1^2} \phi_B^1, \\ D &= \phi_B^3 - \frac{\lambda_1}{K_3^2 - K_2^2} \phi_B^2 + \frac{\lambda_1 \lambda_2}{(K_3^2 - K_2^2)(K_3^2 - K_1^2)} \phi_B^1, \\ E &= \frac{\lambda_2}{K_3^2 - K_1^2} \phi_B^2 - \frac{\lambda_1 \lambda_2}{(K_3^2 - K_2^2)(K_2^2 - K_1^2)} \phi_B^1, \\ F &= \frac{\lambda_1 \lambda_2}{(K_3^2 - K_1^2)(K_2^2 - K_1^2)} \phi_B^1. \end{aligned} \right\} \quad (65)$$

With the continuity condition of the neutron current at $l=0$, the analytical equations in the reflector are combined with the finite difference equations in the core:

$$-D_1^g \frac{\phi_1^g - \phi_{B1}^g}{\Delta r_1/2} = D_R^g \left(\frac{d\phi_R^g}{dl} \right)_{l=0}. \quad (66)$$

For the first energy-group, the boundary flux is obtained as

$$\begin{aligned} D_R^1 \left(\frac{d\phi_R^1}{dl} \right)_{l=0} &= -D_R^1 K_1 \phi_{B1}^1, \\ \phi_{B1}^1 &= \frac{2D_1^1}{D_1^1 K_1 \Delta r_1 + 2D_1^1} \phi_1^1 \equiv \alpha_B \phi_1^1. \end{aligned} \quad (67)$$

For the 2nd energy-group, the boundary flux is

$$\begin{aligned} D_R^2 \left(\frac{d\phi_R^2}{dl} \right)_{l=0} &= D_R^2 (-K_2 B - K_1 C), \\ \phi_{B1}^2 &= \frac{\phi_1^2 + \frac{\Delta r_1}{2D_1^2} \frac{\lambda_1 K_2 - \lambda_1 K_1}{K_2^2 - K_1^2} \phi_{B1}^1}{1 + \frac{K_2 \Delta r_1 D_R^2}{2D_1^2}} = \frac{\phi_1^2 + \beta_B \phi_{B1}^1}{\gamma_B}, \end{aligned} \quad (68)$$

where

$$\begin{aligned} \beta_B &= \frac{\Delta r_1 (\lambda_1 K_2 - \lambda_1 K_1)}{2D_1^2 (K_2^2 - K_1^2)}, \\ \gamma_B &= 1 + \frac{K_2 \Delta r_1 D_R^2}{2D_1^2}. \end{aligned}$$

For the 3rd energy-group, the boundary flux is given by

$$\begin{aligned} D_R^3 \left(\frac{d\phi_R^3}{dl} \right)_{l=0} &= D_R^3 \{-K_3 D - K_2 E - K_1 F\}, \\ \phi_{B1}^3 &= \frac{\phi_1^3 + \tau_B \phi_{B1}^2 + \epsilon_B \phi_{B1}^1}{\phi_B}, \end{aligned} \quad (69)$$

where

$$\begin{aligned} \epsilon_B &= \frac{D_R^3 \Delta r_1 \lambda_1 \lambda_2}{2D_1^3} \cdot \frac{K_3(K_2^2 - K_1^2) + K_2(K_1^2 - K_3^2) + K_1(K_3^2 - K_2^2)}{(K_3^2 - K_2^2)(K_3^2 - K_1^2)(K_2^2 - K_1^2)}, \\ \tau_B &= 1 + \frac{K_3 \Delta r_1 D_R^3}{2D_1^3}. \end{aligned}$$

In core calculation, a finite difference method is applied. The finite difference equation of one-dimensional neutron diffusion at the initial mesh point is expressed as follows:

$$\tilde{D}_1^g \frac{\phi_1^g - \phi_{B1}^g}{(\Delta r_1/2)} - \tilde{D}_1^g (\phi_2^g - \phi_1^g) + D_1^g B_c^g \phi_1^g \Delta r_1 + \Sigma_{T1}^g \phi_1^g \Delta r_1 - d_1^g \Delta r_1 = 0, \quad (70)$$

where

$$\begin{aligned} B_c^g &= \text{the square of a perpendicular buckling in the core,} \\ \Sigma_{Tn}^g &= \Sigma_{an}^g + \Sigma_{rn}^g, \end{aligned}$$

$$d_n^g = \chi^g S_n + \Sigma_{rn}^{g-1} \phi_n^{g-1},$$

χ^g = fission neutron energy spectrum,

S_n = normalized neutron source,

$$\tilde{D}_n^g = \frac{2}{\frac{(\Delta r)_{n-1}}{D_{n-1}} + \frac{(\Delta r)_n}{D_n}},$$

$$\tilde{\tilde{D}}_n^g = \frac{2}{\frac{(\Delta r)_n}{D_n} + \frac{(\Delta r)_{n+1}}{D_{n+1}}}.$$

The finite difference equation for all mesh points except for the initial and end points is expressed as follows:

$$\tilde{D}_n^g(\phi_n^g - \phi_{n-1}^g) + \tilde{\tilde{D}}_n^g(\phi_n^g - \phi_{n+1}^g) + D_n^g B_c^g \phi_n^g \Delta r_n + \Sigma_{Tn}^g \phi_n^g \Delta r_n - d_n^g \Delta r_n = 0. \quad (71)$$

The neutron flux ϕ_n^g can thus be obtained by using the recursion formula:

$$\phi_n^g = \frac{\phi_{n+1}^g + \beta_n^g}{\alpha_n^g}. \quad (72)$$

The coefficients α_n and β_n are obtained by the following recursion formula:

$$\left. \begin{aligned} \alpha_n^g &= k_n^g - \frac{l_n^g}{\alpha_{n-1}^g}, \\ \beta_n^g &= \frac{l_n^g}{\alpha_{n-1}^g} \beta_{n-1}^g + m_n^g, \end{aligned} \right\} \quad (73)$$

where

$$k_n^g \equiv \frac{1}{\tilde{D}_n^g} (\tilde{D}_n^g + \tilde{\tilde{D}}_n^g + \Sigma_{Tn}^g \Delta r_n + D_n^g B_c^g \Delta r_n).$$

$$l_n^g \equiv \frac{\tilde{D}_n^g}{\tilde{\tilde{D}}_n^g},$$

$$m_n^g \equiv \frac{d_n^g \Delta r_n}{\tilde{\tilde{D}}_n^g}.$$

The initial values of α_n^g and β_n^g , e. g. α_1^g and β_1^g , are obtained by substituting Eqs. (67)~(69) to Eq. (70). For the first energy-group, the following equation is obtained by substituting Eq. (67) to Eq. (70).

$$D_1^1 \frac{\phi_1^1 - \alpha_B \phi_1^1}{\Delta r_1/2} - \tilde{\tilde{D}}_1^1 (\phi_2^1 - \phi_1^1) + D_1^1 B_c^1 \phi_1^1 \Delta r_1 + \Sigma_{T1}^1 \phi_1^1 \Delta r_1 - d_1^1 \Delta r_1 = 0.$$

Hence,

$$\left. \begin{aligned} \phi_1^1 &= \frac{\phi_2^1 + \beta_1^1}{\alpha_1^1}, \\ \alpha_1^1 &= \frac{\frac{2}{\Delta r_1} D_1^1 (1 - \alpha_B) + \tilde{\tilde{D}}_1^1 + (\Sigma_{T1}^1 + D_1^1 B_c^1) \Delta r_1}{\tilde{\tilde{D}}_1^1}, \\ \beta_1^1 &= \frac{d_1^1}{\tilde{\tilde{D}}_1^1} \Delta r_1. \end{aligned} \right\} \quad (74)$$

For second energy-group, by substituting Eq. (68) to (70), we get

$$D_1^2 \frac{\phi_2^2 - \phi_2^2 + \beta_B \phi_{B1}^1}{\Delta r_1/2} - \tilde{\tilde{D}}_1^2 (\phi_2^2 - \phi_1^2) + D_1^2 B_c^2 \phi_1^2 \Delta r_1 + \Sigma_{T1}^2 \phi_1^2 \Delta r_1 - d_1^2 \Delta r_1 = 0,$$

$$\phi_1^2 = \frac{\phi_2^2 + \left(d_1^2 \Delta r_1 + \frac{2D_1^2 \beta_B}{\Delta r_1 \gamma_B} \phi_B^1 \right) / \tilde{D}_1^2}{2/\Delta r_1 \cdot D_1^2 \left(1 - \frac{1}{\gamma_B} \right) + \tilde{D}_1^2 + (D_1^2 B_c^2 + \Sigma_{T1}^2) \Delta r_1} \cdot \frac{\tilde{D}_1^2}{\tilde{D}_1^2}.$$

Hence, α_1^2 and β_1^2 are obtained as

$$\left. \begin{aligned} \alpha_1^2 &= \frac{\frac{2}{\Delta r_1} D_1^2 \left(1 - \frac{1}{\gamma_B} \right) + D_1^2 + (D_1^2 B_c^2 + \Sigma_{T1}^2) \Delta r_1}{\tilde{D}_1^2}, \\ \beta_1^2 &= \frac{d_1^2 \Delta r_1 + \frac{2}{\Delta r_1} D_1^2 \frac{\beta_B}{\gamma_B} \phi_B^1}{D_1^2}. \end{aligned} \right\} \quad (75)$$

For the third energy-group, by substituting Eq. (69) to (70), we have

$$\begin{aligned} D_1^3 \frac{\phi_1^3 - \frac{\phi_1^3 + \tau_B \phi_B^2 + \epsilon_B \phi_B^1}{\phi_B}}{\Delta r_1/2} - \tilde{D}_1^3 (\phi_2^2 - \phi_1^3) + D_1^3 B_c^3 \phi_1^3 \Delta r_1 + \Sigma_{T1}^3 \phi_1^3 \Delta r_1 - d_1^3 \Delta r_1 &= 0, \\ \phi_1^3 &= \frac{\phi_2^2 + \left\{ d_1^3 \Delta r_1 + \frac{2D_1^3 (\tau_B \phi_B^2 + \epsilon_B \phi_B^1)}{\Delta r_1 \phi_B} \right\} / \tilde{D}_1^3}{\frac{2}{\Delta r_1} D_1^3 \left(1 - \frac{1}{\phi_B} \right) + \tilde{D}_1^3 + (D_1^3 B_c^3 + \Sigma_{T1}^3) \Delta r_1}, \end{aligned}$$

Hence,

$$\left. \begin{aligned} \alpha_1^3 &= \frac{\frac{2}{\Delta r_1} D_1^3 \left(1 - \frac{1}{\phi_B} \right) + \tilde{D}_1^3 + (D_1^3 B_c^3 + \Sigma_{T1}^3) \Delta r_1}{\tilde{D}_1^3}, \\ \beta_1^3 &= \frac{d_1^3 \Delta r_1 + \frac{2D_1^3 (\tau_B \phi_B^2 + \epsilon_B \phi_B^1)}{\Delta r_1 \phi_B}}{\tilde{D}_1^3}. \end{aligned} \right\} \quad (76)$$

The end values of α_n^g and β_n^g , e.g. α_N^g and β_N^g , are obtained in almost the same manner as the initial values, as follow :

$$\begin{aligned} \tilde{D}_N^g (\phi_N^g - \phi_{N-1}^g) - D_N^g \frac{\phi_{BN}^g - \phi_N^g}{\Delta r_N/2} + D_N^g B_c^g \phi_N^g \Delta r_N + \Sigma_{TN}^g \phi_N^g \Delta r_N - d_N^g \Delta r_N &= 0, \\ \phi_{BN}^g &= \frac{\Delta r_N}{D_N^g} \left(\tilde{D}_N^g + \frac{2D_N^g}{\Delta r_N} + D_N^g B_c^g \Delta r_N + \Sigma_{TN}^g \Delta r_N \right) \phi_N^g. \end{aligned}$$

Hence,

$$\left. \begin{aligned} \alpha_N^g &= K_N^g - \frac{l_N^g}{\alpha_{N-1}^g}, \\ \beta_N^g &= \frac{l_N^g}{\alpha_{N-1}^g} \beta_{N-1}^g + m_N^g, \\ \phi_{N-1}^g &= \frac{\phi_N^g + \beta_{N-1}^g}{\alpha_{N-1}^g}, \\ \phi_{BN}^g &= \alpha_N^g \phi_N^g - \beta_N^g. \end{aligned} \right\} \quad (77)$$

At the end mesh point in core ($l^*=0$), the neutron current must satisfy the continuity condition :

$$-D_N^g \frac{\phi_{BN}^g - \phi_N^g}{\Delta r_N/2} = -D_R^g \left(\frac{d\phi_R^g}{dl^*} \right)_{l^*=0}. \quad (78)$$

Therefore, for the 1st energy-group, we get from Eqs. (64) and (65),

$$-D_R^1 \left(\frac{d\phi_B^1}{dl^*} \right)_{l^*=0} = D_R^1 K_1 \phi_{BN}^1. \quad (79)$$

Using the Eqs. (79), (78) and (77) given above, the following initial value of Eq. (77) is obtained :

$$\phi_N^1 = \frac{\frac{2D_N^1}{\Delta r_N} \beta_N^1 + D_R^1 K_1 \beta_N^1}{\frac{2D_N^1}{\Delta r_N} (\alpha_N^1 - 1) + D_R^1 K_1 \alpha_N^1} , \quad (80)$$

For the 2nd energy-group, in same manner as for the 1st group,

$$\begin{aligned} -D_N^2 \frac{\phi_{BN}^2 - \phi_N^2}{\Delta r_N / 2} &= -D_R^2 \left(\frac{d\phi_R^2}{dl^*} \right)_{l^*=0} = D_R^2 K_2 \left(\phi_{BN}^2 - \frac{\lambda_1}{K_2^2 - K_1^2} \phi_{BN}^1 \right) \\ &+ D_R^2 K_1 \frac{\lambda_1}{K_2^2 - K_1^2} \phi_{BN}^1 . \end{aligned}$$

Hence

$$\phi_N^2 = \frac{\frac{2D_N^2}{\Delta r_N} \beta_N^2 + D_R^2 K_2 \left(\beta_N^2 + \frac{\lambda_1}{K_2^2 - K_1^2} \phi_{BN}^1 \right) - D_R^2 K_1 \frac{\lambda_1}{K_2^2 - K_1^2} \phi_{BN}^1}{\frac{2D_N^2}{\Delta r_N} (\alpha_N^2 - 1) + D_R^2 K_2 \alpha_N^2} . \quad (81)$$

For the 3rd energy-group,

$$\begin{aligned} -D_N^3 \frac{\phi_{BN}^3 - \phi_N^3}{\Delta r_N / 2} &= -D_R^3 \left(\frac{d\phi^3}{dl^*} \right)_{l^*=0} \\ &= D_R^3 (K_3 D + K_2 E + K_1 F) \\ &= D_R^3 K_3 \phi_{BN}^3 - \frac{D_R^2 (K_3 - K_2) \lambda_2}{K_3^2 - K_2^2} \phi_{BN}^2 \\ &+ \frac{D_R^3 K_3 \lambda_1 \lambda_2 \{ K_3 (K_2^2 - K_1^2) - K_2 (K_3^2 - K_2^2) + K_1 (K_3^2 - K_2^2) \}}{(K_3^2 - K_1^2)(K_2^2 - K_1^2)(K_3^2 - K_2^2)} \phi_{BN}^1 . \end{aligned}$$

Hence,

$$\begin{aligned} \phi_N^3 &= \frac{\frac{2D_N^3}{\Delta r_N} \beta_N^3 + D_R^3 K_3 \beta_N^3 + \xi_B}{\frac{2D_N^3}{\Delta r_N} (\alpha_N^3 - 1) + D_R^3 K_3 \alpha_N^3} , \quad (82) \\ \xi_B &= \frac{D_R (K_3 - K_2) \lambda_2}{K_3^2 - K_2^2} \phi_{BN}^2 \\ &- \frac{D_R^2 K_3 \lambda_1 \lambda_2 \{ K_3 (K_2^2 - K_1^2) - K_2 (K_3^2 - K_1^2) + K_1 (K_3^2 - K_2^2) \}}{(K_3^2 - K_1^2)(K_2^2 - K_1^2)(K_3^2 - K_2^2)} \phi_{BN}^1 . \end{aligned}$$

Next we explain the method to calculate the two-dimensional neutron flux at the core boundary in a XY plane. The two-dimensional neutron diffusion equation is expressed as follows :

$$-D^g(r) \nabla^2 \phi^g(r) + \Sigma_T^g(r) \phi^g(r) = X^g S(r) + \Sigma_r^{g-1}(r) \phi_{(r)}^{g-1} , \quad (83)$$

where

$$\begin{aligned} S(r) &= \frac{1}{\lambda} \sum_g \nu \Sigma_f^g(r) \phi^g(r) , \\ \Sigma_T^g(r) &= \Sigma_a^g(r) + \Sigma_r^g(r) + L_z^g(r) . \end{aligned}$$

A two-dimensional region is divided into K intervals along X axis and L intervals along Y axis. Any node in the region is identified by (k, l) . The widths of left, right, front and back sides are expressed by the notations L , R , T and B , respectively. Each phase around the point (k, l) is identified by 1, 2, 3 or 4 as shown in Fig. 7. The node point $P(k, l)$ is expressed by Cartesian co-ordinate (ξ_p, τ_p) and the diffusion equation (83) is integrated over the following small intervals :

$$\begin{aligned} \xi_p - \frac{L}{2} \leq \xi \leq \xi_p + \frac{R}{2} , \\ \tau_p - \frac{B}{2} \leq \tau \leq \tau_p + \frac{T}{2} . \end{aligned}$$

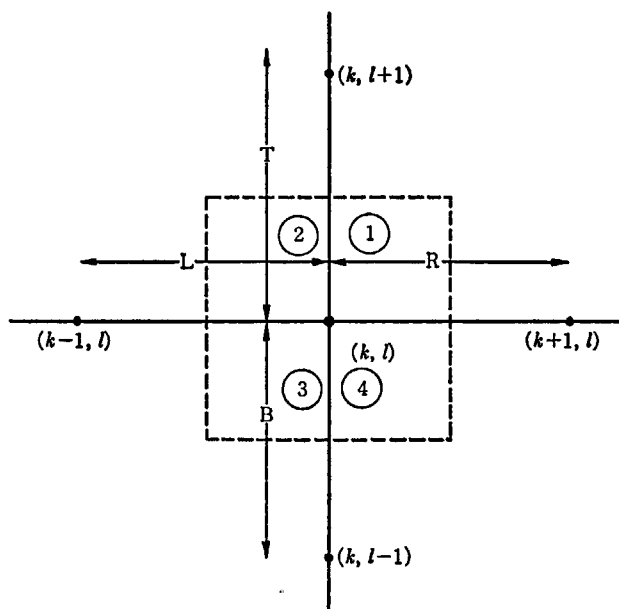


Fig. 7 Mesh interval in two-dimensional calculation.

The material in each phase belonged to a node point $P(k, l)$ may be different from each other and the nuclear constants in each phase are expressed as $\Sigma^i(P)$ ($i=1, 2, 3, 4$).

The neutron flux and neutron current at the boundary plane containing the node point $P(k, l)$ must be continuous:

$$\phi_{\xi-}(P) = \phi_{\xi+}(P) ,$$

$$\phi_{\tau-}(P) = \phi_{\tau+}(P) ,$$

$$J_{\xi-}(P) = J_{\xi+}(P) ,$$

$$J_{\tau-}(P) = J_{\tau+}(P) .$$

By integrating Eq. (83) and using the above relations, and the first term on the left side of Eq. (83) becomes as follows:

$$\begin{aligned} -\iint D\nabla^2 \phi dS &= -\int D\nabla \phi ds \\ &= -\left\{ \frac{D_1}{R} \left(\frac{T}{2} \right) + \frac{D_4}{R} \left(\frac{B}{2} \right) \right\} (\phi_{k+1,l} - \phi_{k,l}) \\ &\quad - \left\{ \frac{D_2}{T} \left(\frac{L}{2} \right) + \frac{D_1}{T} \left(\frac{R}{2} \right) \right\} (\phi_{k,l+1} - \phi_{k,l}) \\ &\quad - \left\{ \frac{D_2}{L} \left(\frac{T}{2} \right) + \frac{D_3}{L} \left(\frac{B}{2} \right) \right\} (\phi_{k-1,l} - \phi_{k,l}) \\ &\quad - \left\{ \frac{D_3}{B} \left(\frac{L}{2} \right) + \frac{D_4}{B} \left(\frac{R}{2} \right) \right\} (\phi_{k,l-1} - \phi_{k,l}) \end{aligned}$$

The second term on the left side and the right side of Eq. (83) give

$$\begin{aligned} \iint \Sigma_T \phi ds &= \left\{ \Sigma_{T1} \cdot \frac{TR}{4} + \Sigma_{T2} \frac{LT}{4} + \Sigma_{T3} \frac{LB}{4} + \Sigma_{T4} \frac{RB}{4} \right\} \phi_{k,l} , \\ \iint f ds &= f_1 \frac{TR}{4} + f_2 \frac{LT}{4} + f_3 \frac{LB}{4} + f_4 \frac{RB}{4} , \end{aligned}$$

where $f_q = X^q S_{k,l,q} + \Sigma_{Tq} g^{-1} \phi_{k,l} g^{-1}$.

Using the above results, Eq. (83) is expressed as a following five points difference equation:

$$-(a_{k,l} \phi_{k+1,l} + b_{k,l} \phi_{k,l-1} + c_{k,l} \phi_{k-1,l} + d_{k,l} \phi_{k,l+1}) + P_{k,l} \phi_{k,l} = f_{k,l} , \quad (84)$$

where

$$\left. \begin{aligned} a_{k,l} &= \left\{ \frac{D_1 T + D_4 B}{2} \right\} / R, \\ b_{k,l} &= \left\{ \frac{D_3 L + D_4 R}{2} \right\} / B, \\ c_{k,l} &= \left\{ \frac{D_3 T + D_3 B}{2} \right\} / L, \\ d_{k,l} &= \left\{ \frac{D_2 L + D_1 R}{2} \right\} / T, \\ \gamma_{k,l} &= \left\{ \frac{\Sigma_{T1} R}{2} + \frac{\Sigma_{T2} L}{2} \right\} \frac{T}{2} + \left\{ \frac{\Sigma_{T3} L}{2} + \frac{\Sigma_{T4} R}{2} \right\} \frac{B}{2}, \\ P_{k,l} &= a_{k,l} + b_{k,l} + c_{k,l} + d_{k,l} + \gamma_{k,l}, \\ f_{k,l} &= \left\{ \frac{f_1 R}{2} + \frac{f_2 L}{2} \right\} \frac{T}{2} + \left\{ \frac{f_3 L}{2} + \frac{f_4 R}{2} \right\} \frac{B}{2}, \end{aligned} \right\} \quad (85)$$

Now, we consider the expression of the neutron flux at the left side boundary between the reflector and the core.

For the first energy-group, by using the boundary neutron flux $\phi_{0,l}$, the neutron current from the core, J_c^1 is given by

$$\begin{aligned} J_c^1 &= \frac{D_2^1}{L} \cdot \frac{T}{2} \cdot (\phi_{1,l^1} - \phi_{0,l^1}) + \frac{D_3^1}{L} \cdot \frac{B}{2} \cdot (\phi_{1,l^1} - \phi_{0,l^1}) \\ &= \frac{(D_2^1 T + D_3^1 B) \phi_{1,l^1} - \phi_{0,l^1}}{L}. \end{aligned} \quad (86)$$

From Eqs. (64) and (65), the neutron current from the reflector, J_R^1 , is expressed as follows:

$$J_R^1 = \left(-D_R^1 \frac{\partial \phi^1}{\partial l} \right)_{l=0} \left(\frac{T+B}{2} \right) = K_1 D_R^1 \phi_{B^1} \left(\frac{T+B}{2} \right).$$

The continuity conditions of the neutron current ($J_c^1 = J_R^1$) and the neutron flux ($\phi_{B^1} = \phi_{0,l^1}$) must be satisfied:

$$\frac{D_2^1 T + D_3^1 B \phi_{1,l^1} - \phi_{0,l^1}}{L} = K_1 D_R^1 \phi_{0,l^1} \left(\frac{T+B}{2} \right). \quad (87)$$

Hence, $\phi_{0,l^1} = u^{(1)} \cdot \phi_{1,l^1}$,

where

$$u^{(1)} = \frac{1}{1 + \frac{D_R^1 (T+B)}{(D_2^1 T + D_3^1 B)}}.$$

Equation (84) at the left boundary of the core is expressed as follows:

$$-(a_{1,l} \phi_{2,l} + b_{1,l} \phi_{1,l-1} + d_{1,l} \phi_{1,l+1}) + (P_{1,l} - u^{(1)} \cdot c_{1,l}) \phi_{1,l} = f_{1,l}. \quad (89)$$

As shown above, in our computer program the element $P_{1,l}$ of the coefficient matrix of the normal five mesh point difference Equation (84) is corrected to $(P_{1,l} - u^{(1)} \cdot c_{1,l})$ and then $c_{1,l}$ of Eq. (85) is set to be zero.

For the second energy-group by using Eqs. (64) and (65), the neutron current from the reflector is expressed as follows:

$$\begin{aligned} -D_R^2 \left(\frac{\partial \phi^2}{\partial l} \right)_{l=0} \cdot \frac{T+B}{2} &= \left\{ D_R^2 K_2 \left(\phi_{0,l^2} - \frac{\lambda_1}{K_2^2 - K_1^2} \phi_{0,l^1} \right) + D_R^2 K_1 \frac{\lambda_1}{K_2^2 - K_1^2} \phi_{0,l^1} \right\} \\ &\quad \times \frac{T+B}{2}. \end{aligned}$$

Therefore,

$$\frac{D_2^2 T + D_3^2 B \phi_{1,l^2} - \phi_{0,l^2}}{L} = \frac{D_R^2 (T+B)}{2} \left\{ K_2 \phi_{0,l^2} - \frac{\lambda_1}{K_2 + K_1} \phi_{0,l^1} \right\}.$$

Hence,

$$\begin{aligned}\phi_{0,i^2} &= \frac{1}{1 + \frac{D_R^2(T+B)}{D_2^2T + D_3^2B} - K_2L} \phi_{1,i^2} + \frac{LD_R^2(T+B) \frac{\lambda_1}{K_1+K_2}}{D_R^2(T+B)K_1L + (D_2^2T + D_3^2B)} \phi_{0,i^1} \\ &= u^{(2)} \phi_{1,i^2} + V^{(2)} \phi_{0,i^1},\end{aligned}\quad (90)$$

where

$$\begin{aligned}u^{(2)} &= \frac{1}{1 + \frac{D_R^2(T+B)}{D_2^2T + D_3^2B} K_2L}, \\ V^{(2)} &= \frac{LD_R^2(T+B) \frac{\lambda_1}{K_1+K_2}}{D_R^2(T+B)K_2L + (D_2^2T + D_3^2B)}.\end{aligned}$$

In the above equation, the boundary flux at the first energy-group ϕ_{0,i^1} has been obtained by Eq. (87). In our programing, the term $-u^{(2)} \cdot c_{1,i}$ is added to the element $P_{1,i}$ of the coefficient matrix, $V^{(2)} c_{1,i}$ is added to $f_{1,i}$ and then $c_{1,i}$ is set to be zero.

For the third energy-group, from Eqs. (64) and (65), the neutron current from the reflector is expressed as follows:

$$\begin{aligned}-D_R^2 \left(\frac{d\phi^3}{dl} \right)_i \cdot \left(\frac{T+B}{2} \right) &= \frac{(T+B)}{2} D_R \times \{K_3D + K_2E + K_1F\} \\ &= \frac{T+B}{2} D_R^3 \times \left[K_3\phi_{0,i^3} - \frac{\lambda_2}{K_3+K_2} \phi_{0,i^2} \right. \\ &\quad \left. + \phi_{0,i^1} \cdot \frac{\lambda_1\lambda_2 \{K_3(K_2^2 - K_1^2) - K_2(K_3^2 - K_1^2) + K_1(K_3^2 - K_2^2)\}}{(K_3^2 - K_2^2)(K_3^2 - K_1^2)(K_2^2 - K_1^2)} \right].\end{aligned}$$

By using the continuity condition of the neutron current, the neutron flux at the boundary ϕ_{0,i^3} is obtained as follows:

$$\begin{aligned}\frac{(D_2^3T + D_3^3B)(\phi_{1,i^3} - \phi_{0,i^3})}{2} &= \frac{(T+B)D_R^3}{2} \left[K_3\phi_{0,i^3} - \frac{\lambda_2}{K_3+K_2} \phi_{0,i^2} \right. \\ &\quad \left. + \frac{\lambda_1\lambda_2 \{K_3(K_2^2 - K_1^2) - K_2(K_3^2 - K_1^2) + K_1(K_3^2 - K_2^2)\}}{(K_3^2 - K_2^2)(K_3^2 - K_1^2)(K_2^2 - K_1^2)} \phi_{0,i^1} \right].\end{aligned}$$

Hence,

$$\phi_{0,i^3} = u^{(3)} \phi_{1,i^3} + V^{(3)} \phi_{0,i^2} + W^{(3)} \phi_{0,i^1}, \quad (91)$$

where

$$\begin{aligned}u^{(3)} &= \frac{1}{1 + \frac{D_R^3(T+B)}{D_2^3T + D_3^3B} K_3L}, \\ V^{(3)} &= \frac{LD_R^3(T+B) \frac{\lambda_2}{K_2+K_3}}{D_R^3(T+B)K_3L + (D_2^3T + D_3^3B)}, \\ W^{(3)} &= \frac{LD_R^3(T+B) \frac{\lambda_1\lambda_2 \{K_3(K_2^2 - K_1^2) - K_2(K_3^2 - K_1^2) + K_1(K_3^2 - K_2^2)\}}{(K_3^2 - K_2^2)(K_3^2 - K_1^2)(K_2^2 - K_1^2)}}{D_R^3(T+B)K_3L + (D_2^3T + D_3^3B)}.\end{aligned}$$

Hence, Eq. (84) is expressed as

$$\begin{aligned}&-(a_{1,i}\phi_{2,i^3} + b_{1,i}\phi_{1,i-1^3} + d_{1,i}\phi_{1,i+1^3}) + (P_{1,i} - u^{(3)}c_{1,i})\phi_{1,i^3} \\ &= f_{1,i} + V^{(3)}c_{1,i} + W^{(3)}c_{1,i}\phi_{0,i^1}.\end{aligned}\quad (92)$$

In our programing, the term $-u^{(3)} \cdot c_{1,i}$ is added to the element $P_{1,i}$ of the coefficient matrix, $(V^{(3)}c_{1,i}\phi_{0,i^2} + W^{(3)}c_{1,i}\phi_{0,i^1})$ is added to $f_{1,i}$ and then $c_{1,i}$ is set to be zero.

On the other sides of the boundary, the coefficient matrix is obtained in exactly the same manner.

3. Test Calculations

Numerical calculations were made with the DIFFUSION-ACE code for the reactor core shown in Fig. 8. The section of a block is 12×12 cm, which is slightly smaller than that of a usual fuel bundle for boiling water reactors. The core is divided into two material regions. Region I contains a strong absorber and Region II does not.

The four kind of mesh intervals, $\Delta x (= \Delta y = \Delta z) = 12, 6, 4$ and 2 cm were adopted. The total number of neutron energy-groups was three. For comparison, the computer code ADC⁵⁾ which adopts the standard fine-mesh difference approximation method was also used for these calculations.

The results of calculations follow :

- 1) TABLE 1 shows the neutron leakage from each block. The neutron leakage is distributed three-dimensionally.
- 2) The eigenvalues obtained for various mesh widths are summarized in TABLE 2. If the exact eigenvalues is assumed to be 1.1255, the results by the present code is 0.15% larger than the exact value. However the difference is so small that the results are considered to be in a good agreement with that obtained by the ADC code.
- 3) In Fig. 9, the thermal neutron flux distributions along the Z axis at channel 1 is compared with that calculated by the ADC code. The results by DIFFUSION-ACE show channel-integrated fluxes and hence the solid line should represent the average of the point fluxes by ADC. The point \circ , \triangle and \times in Fig. 9 describe the neutron fluxes at the upper right corner, the lower left corner and the lower right corner of channel 1, respectively, as shown in the diagram in the figure. The both results are shown to be in a good agreement.
- 4) In TABLE 3 is shown the convergence history of the iteration scheme of DIFFUSION-ACE. Both the inner iteration and the combination of the inner and the outer iteration result in the convergence of the eigenvalue.

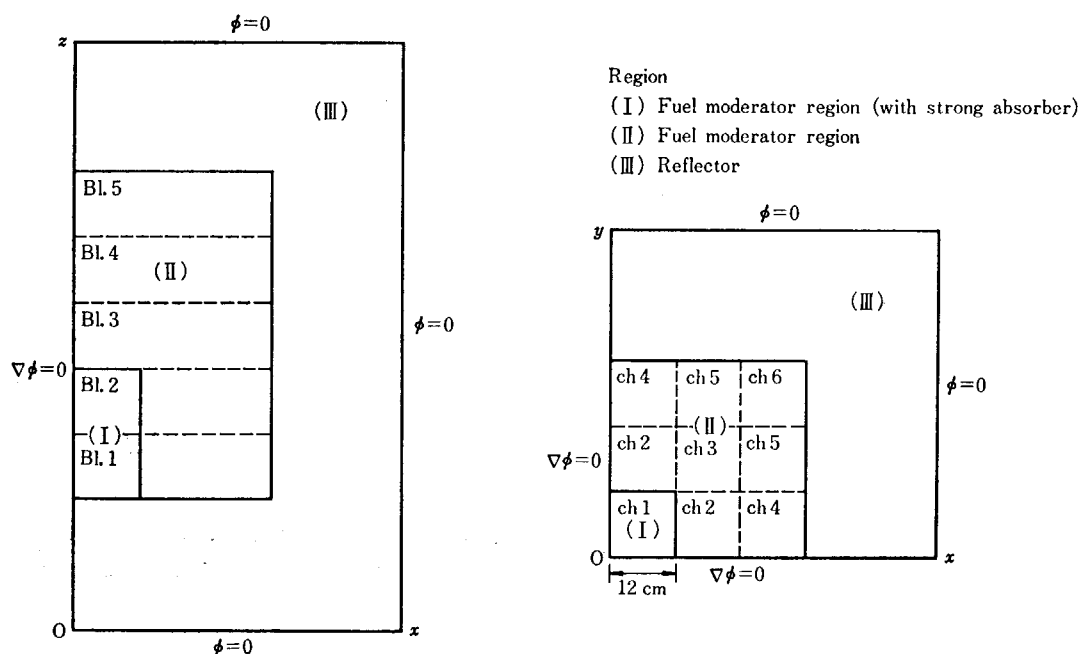


Fig. 8 Configuration for the check calculation.

TABLE 1 Neutron leakage distribution calculated by the DIFFUSION-ACE code at mesh width $\Delta x = \Delta y = \Delta z = 2$ cm

Channel No. 1						
Block No.	L_{x-1G}^a	L_{x-2G}	L_{x-3G}	L_{xy-1G}^c	L_{xy-2G}	L_{xy-3G}
1	0.83996E-02 ^b	0.18677E-02	-0.53751E-02	0.38970E-02	0.17654E-02	0.72240E-03
2	0.36950E-02	0.16729E-02	0.67087E-03	0.37650E-02	0.17073E-02	0.69995E-03
3	0.38938E-02	0.27806E-02	0.15437E-02	0.28502E-02	0.11370E-02	0.39228E-03
4	-0.51401E-03	-0.20132E-02	-0.18460E-02	0.50583E-03	-0.31031E-02	-0.29831E-02
5	0.46154E-02	-0.11543E-03	-0.68900E-02	-0.13801E-02	-0.43332E-02	-0.36464E-02

Channel No. 2						
Block No.	L_{x-1G}	L_{x-2G}	L_{x-3G}	L_{xy-1G}	L_{xy-2G}	L_{xy-3G}
1	0.82919E-02	0.18228E-02	-0.53905E-02	0.39830E-02	0.18055E-02	0.76513E-03
2	0.35177E-02	0.16083E-02	0.65513E-03	0.39317E-02	0.17846E-02	0.72068E-03
3	0.31582E-02	0.15211E-02	0.67025E-03	0.41500E-02	0.38379E-02	0.82681E-03
4	0.12998E-02	0.45610E-03	0.10264E-03	0.49640E-02	0.38379E-02	0.22115E-02
5	0.53817E-02	0.53846E-03	-0.58008E-02	0.53652E-02	0.40200E-02	0.22991E-02

Channel No. 4						
Block No.	L_{x-1G}	L_{x-2G}	L_{x-3G}	L_{xy-1G}	L_{xy-2G}	L_{xy-3G}
1	0.82184E-02	0.17770E-02	-0.48650E-02	0.96783E-02	0.18904E-02	-0.55048E-02
2	0.32815E-02	0.14869E-02	0.62615E-03	0.98003E-02	0.19745E-02	-0.60292E-02
3	0.27706E-02	0.12540E-02	0.50996E-03	0.10364E-01	0.22170E-02	-0.59758E-02
4	0.21418E-02	0.97196E-03	0.42223E-03	0.11055E-01	0.24923E-02	-0.59518E-02
5	0.61811E-02	0.89731E-03	-0.50590E-02	0.11767E-01	0.27714E-02	-0.53591E-02

^a L_{x-1G} =neutron leakage coefficients in the energy group 1 from each block along the x axis.^b Read as 0.83996×10^{-2} .^c L_{xy-1G} =neutron leakage coefficients in the energy group 1 from each block in the xy layer.

TABLE 2 Eigenvalues calculated by the DIFFUSION-ACE and ADC code

Mesh width (cm)	Eigenvalue	
	DIFFUSION-ACE	ADC
2	1.1272	
4	1.1285	1.1255
6	1.1302	1.1272
12	1.1313	1.1430

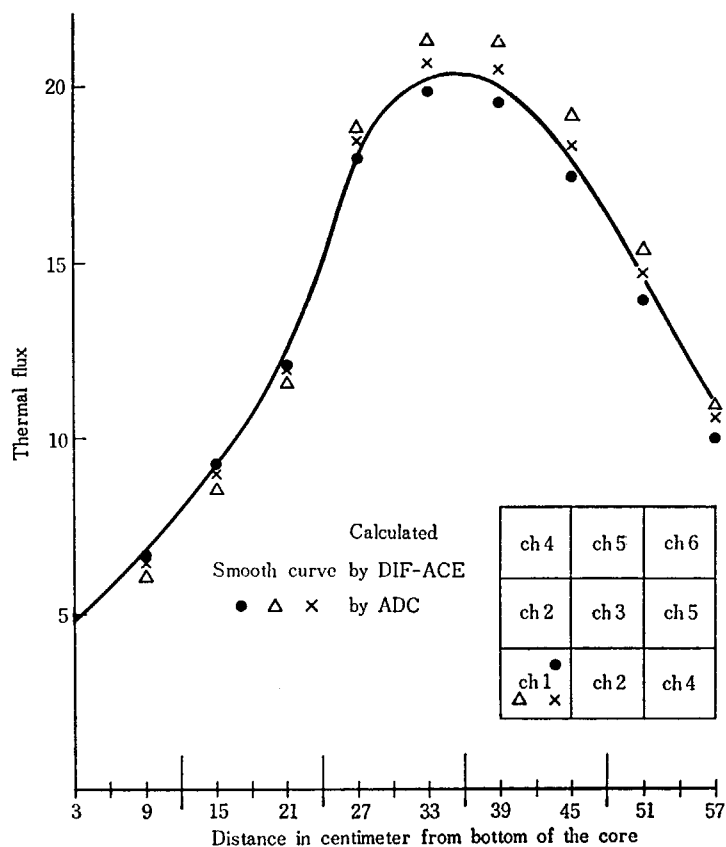


Fig. 9 Comparison of the vertical thermal-neutron flux traverses calculated by the DIFFUSION-ACE and ADC codes. The locations of the traverses within the channel are shown in the diagram.

TABLE 3 Convergence history of the iteration scheme

The sequence number of outer iteration	The number of inner iteration			Eigenvalue
	Energy groups			
	1st	2nd	3rd	
1	9	3	3	1.09721
2	4	3	2	1.13017
3	3	2	2	1.12849
4	2	2	2	1.12792
6	2	1	1	1.12740
8	2	1	1	1.12723
10	2	1	1	1.12719
15	1	1	1	1.12717
20	1	1	1	1.12718
25	1	1	1	1.12718
28	1	1	1	1.12718

4. Guide to User

In this section we provide the information needed for the user to understand DIFFUSION-ACE options and to prepare the input.

4.1 Overall program flow

The program DIFFUSION-ACE is constructed from three main parts, each of which consists of two subprograms, ONEDIM and TWODIM for calculating one- and two-dimensional neutron diffusion equations, respectively.

The first part of the program is a routine to generate an initial guess of the neutron source distribution. To estimate the three-dimensional initial source distribution, a one-dimensional neutron flux and source calculation is performed at each channel along the Z axis by ONEDIM (1) and a two-dimensional neutron flux and source calculation is performed by TWODIM (1) in a layer whose nuclear group constants are obtained by averaging the group constants of all layers along the Z axis using the results of ONEDIM (1). One- and two-dimensional neutron sources are superposed to give a three-dimensional source guess.

The second part is a routine to calculate the neutron flux distribution with a fixed neutron source distribution. This part is constructed from two sub-routines, ONEDIM (2) and TWODIM (2). In ONEDIM (2), the axial leakage L_z and the axial flux ϕ_z are computed with the radial leakage L_{xy} obtained by TWODIM (2). In TWODIM (2), L_{xy} and ϕ_{xy} are calculated using L_z . The one- and two-dimensional leakages are iterated until the consistency is attained between the two. This step of calculation is performed for each energy-group and referred to as inner iteration.

The third part is a routine to calculate the neutron source distribution in the core with the neutron flux obtained in the second part. This routine is referred to as outer iteration or source iteration, and constructed from two subroutines, ONEDIM (3) and TWODIM (3). The check of the convergence is performed by comparing the effective multiplication factor in each block.

General flow chart of the program DIFFUSION-ACE, and the flow charts of the subroutines ONEDIM and TWODIM are shown in Figs. 10, 11 and 12, respectively.

4.2 Discretization of spatial variables

Only orthogonal coordinate X-Y-Z is allowable in this program. The reactor is divided doubly into blocks and meshes. A parallelepiped formed by a channel and a layer is called a block in which the materials are homogenized. A block is sub-divided into fine meshes, and the fine-mesh difference approximation method is applied to solve the one- and two-dimensional neutron diffusion equations for each channel and layer, respectively. It is possible to have mesh-points in the reflector for solving numerically the diffusion equations.

The first step for discretizing the spatial variables is to divide the X-Y plane of the reactor into channels as shown in Fig. 13 and each channel is numbered. The channels which are in the same physical condition are indexed with the same channel number. One-dimensional calculation is performed on each channel number. The second step is to divide the X-Y plan into meshes for solving two-dimensional diffusion equations. In this stage, the numbers of meshes are determined for each channel and for side reflectors. The third step is to divide a channel into blocks

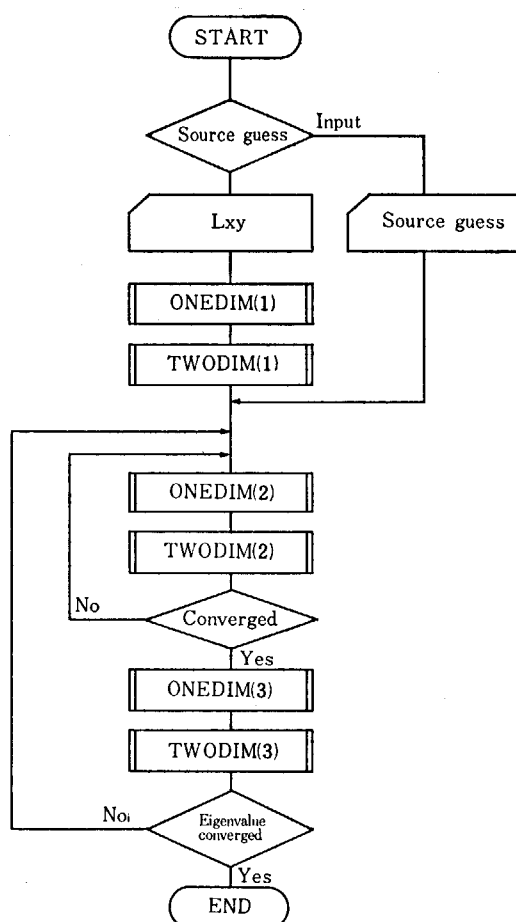


Fig. 10 General flow of DIFFUSION-ACE

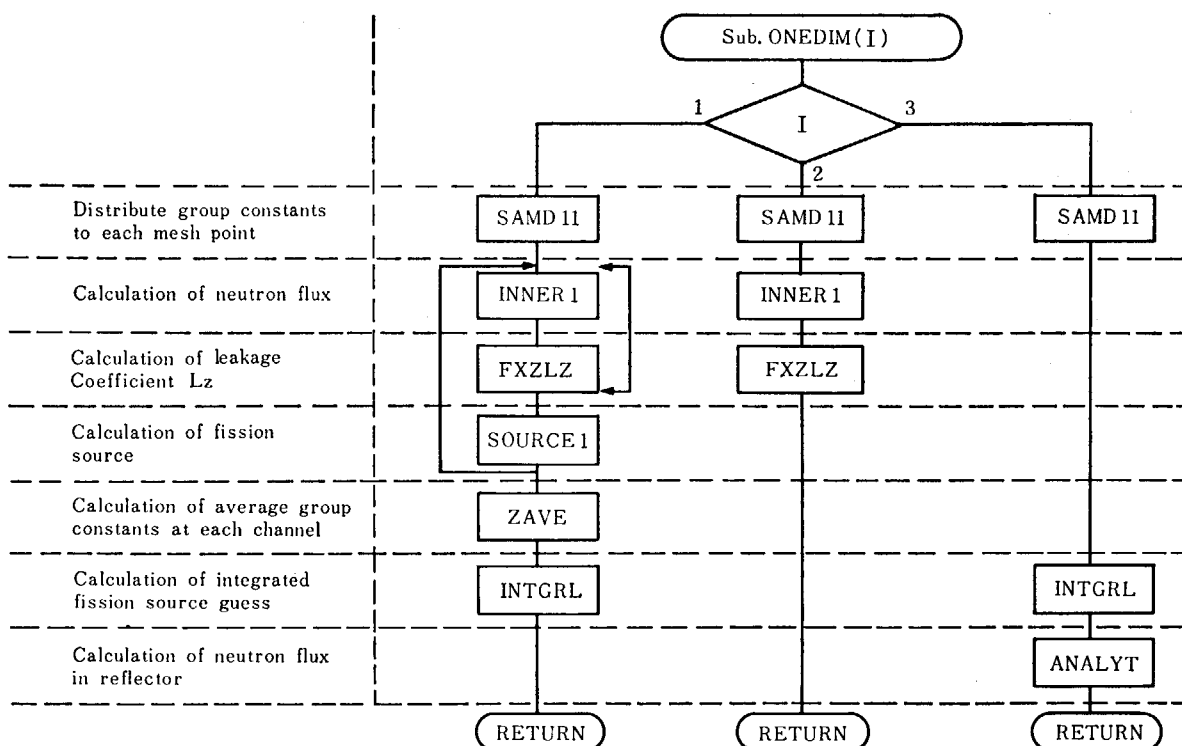


Fig. 11 Flow of subroutine ONEDIM

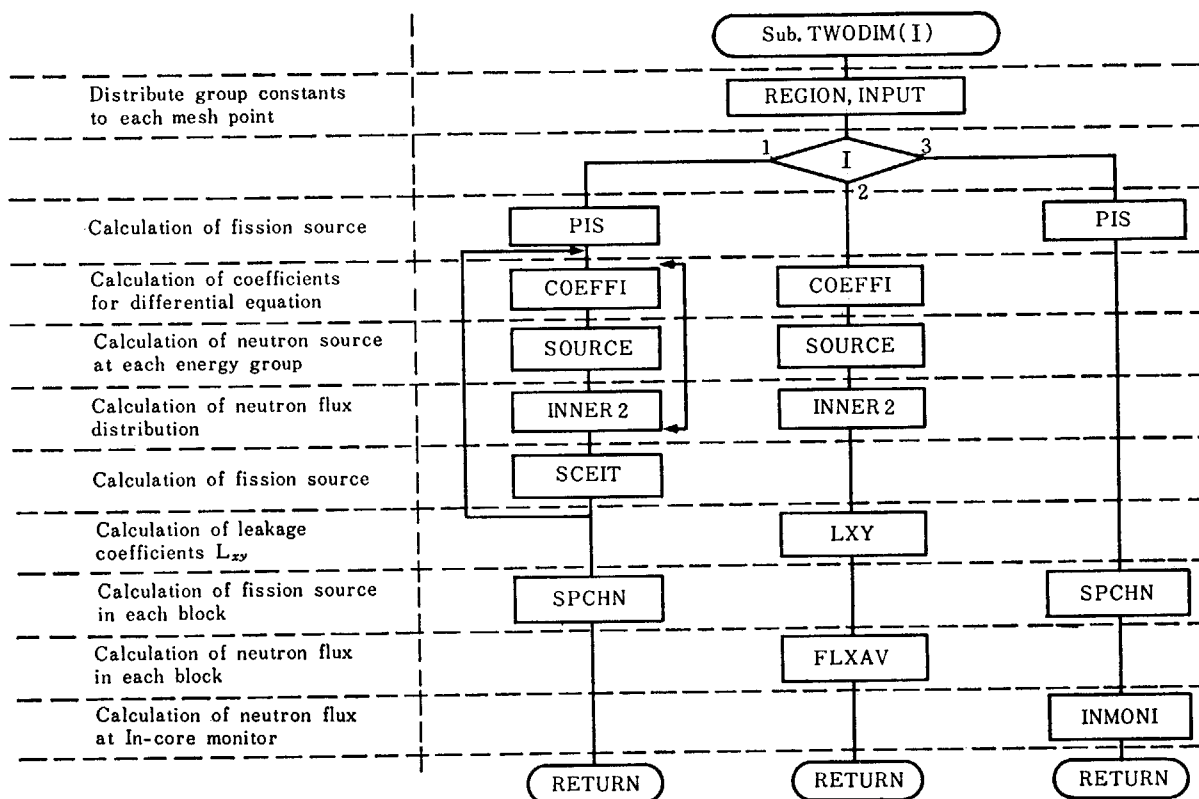
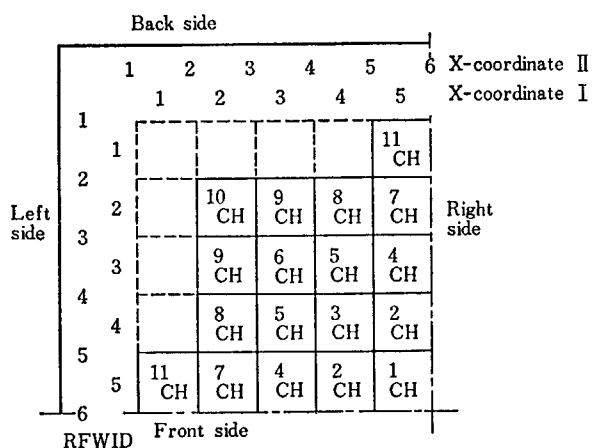


Fig. 12 Flow of subroutine TWODIM



X coordinate I... Coordinate for the specification of the position of channels

X coordinate II... Coordinate for the specification of the position of control rods and in-core monitors.

Y coordinates are similar to those of X.

Fig. 13 X-Y section of the calculational geometry (Example: JPDR 1/4 core)

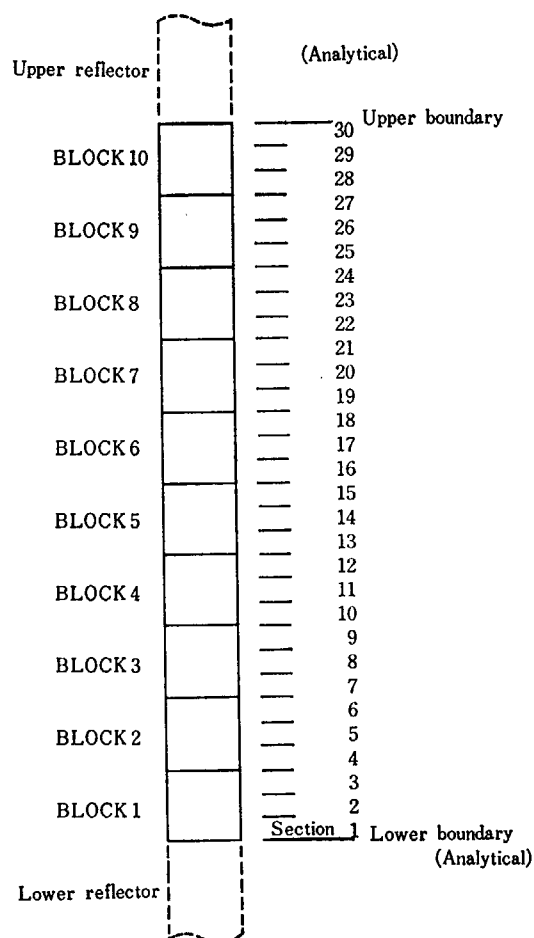


Fig. 14 Z section of a channel. (Example 1)

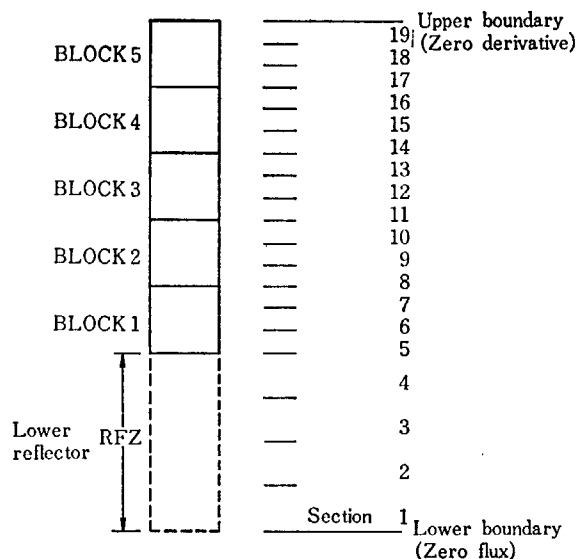


Fig. 15 Z section of a channel. (Example 2)

and sections (or meshes) as shown in Figs. 14 and 15. The case shown in Fig. 14 is that the neutron fluxes in upper and lower reflectors are calculated analytically and the fine-mesh difference approximation method is applied only to the core. On the other hand, in the case shown in Fig. 15, the neutron flux in the lower reflector is computed by the finite difference method.

4.3 Description of input data

The input data for DIFFUSION-ACE are read in I3 format for the integer type and E10.0 format for the floating-point type, in the following order:

Card number	Column	Variable name	Comments
CARD 1	1~3	NPROB	Problem number.
			If not positive, calculation is terminated.
CARD 2	1~72	MTITLE	Job title card in 18A4 format.
CARD 3	1~3	IMAX	Maximum number of channels along X axis (<10).
	4~6	JMAX	Maximum number of channels along Y axis (<10).
	7~9	KMAX	Maximum number of blocks along Z axis (<12).
	10~12	NMAX	Maximum value of channel number at which one-dimensional calculation is performed (<79).
	13~15	ISECT	Number of mesh-points in a channel along X axis.
	16~18	JSECT	Number of mesh-points in a channel along Y axis.
	19~21	KSECT	Number of sections in a block along Z axis.
	22~24	NRMIV	Number of meshes in reflector in the X-Y plane.
	25~27	NRZ	Number of sections in reflector for one-dimensional calculation (for example, NRZ=0 for Fig. 14, NRZ=4 for Fig. 15).
CARD 4	1~3	NCROD	Number of control rods (<16).
	4~6	INMMAX	Number of in-core monitors (<30).
	7~9	NSKO	Number of sections which are subdivided into three subsections with widths of 1/3 of the original width.

Card number	Column	Variable name	Comments
CARD 4	10~12	MNZ	In the case of analytical boundary condition (see CARD 11), number of positions at which the neutron fluxes printed.
	13~15	IGS	Initialization of neutron source distribution. =0 Initial guess of L_{xy} is supplied by input cards and initial source distribution is calculated in the code. =1 Initial source distribution is supplied by input cards (see CARD 26 and 27). =2 Initial source distribution is supplied by disk or tape.
	16~18	KKK	Option to input the diffusion parameters of the core (see CARD 29). =1 Diffusion parameters are the same in the full core. =2 Diffusion parameters are supplied channel-wise. =3 Diffusion parameters are supplied block-wise. =4 Blocks are grouped into some types and diffusion parameters are supplied type-wise.
	19~21	NGMAX	Number of energy-groups which must be two or three.
	22~24	IPUNCH	Output option. =0 No punch output. =1 Neutron source distributions are punched out (see CARD 25, 26 and 27). =2 L_{xy} at each block is punched out. =3 Both neutron source and L_{xy} are punched out. =-1 Neutron source distributions in channels and in layers are written in disk or tape. =-2 L_{xy} at each block is written in disk or tape. =-3 L_{xy} and neutron source distribution are written in disk or tape.
	25~27	ILXY	Input option of initial guess of L_{xy} . =0 Initial guess of L_{xy} is prepared by CARD 29. =1 Initial guess of L_{xy} is prepared by CARD 30 and 31. In this case, L_{xy} prepared by CARD 29 is not used. =2 Initial guess of L_{xy} is prepared by disk or tape.
	1~10	DX	One channel width along X axis (cm).
	11~20	DY	One channel width along Y axis (cm).
	21~30	DZ	One block length along Z axis (cm).
	31~40	RFWID	Reflector width in X-Y plane (cm).
CARD 5	41~50	CRWID	Cross-type control rod thickness in X-Y plane (cm).
	51~60	REFZ	Reflector thickness along Z axis (cm).
	(24I3)	NC(I, J)	Channel number allocated in X-Y plane. Number of input cards (NC(I, J), I=1, IMAX) used in JMAX. The subscripts I and J correspond to X-COORDINATED I and Y-COORDINATE J, respectively, as shown in Fig. 13.

Card number	Column	Variable name	Comments
CARD 7	(8I3, 6X, E10.0)		Identification of control rod. If NCROD=0, this card is not required.
	1~3		Control rod number.
	4~6		Location of a control-rod in X-COORDINATE II (see Fig. 13).
	7~9		Location of a control-rod in Y-COORDINATE II (see Fig. 13).
	10~12 } 13~15 } 16~18 } 19~21 }		Four channel numbers around a control-rod (the order is arbitrary). If there are same numbers, repeat them.
	22~24		Block number which contains the top of a control-rod.
	25~30		Blank.
	31~40		Height of control-rod from the bottom of the core. (cm)
	CARD 7 is repeated NCRD times.		
CARD 8			In-core monitor specification (not required if INMMAX ≤ 0).
	1~3		In-core monitor number.
	4~6		Location of a in-core monitor in X-COORDINATE II.
	7~9		Location of a in-core monitor in Y-COORDINATE II.
	CARD 8 is repeated INMMAX times.		
CARD 9	(24I3)	NSPNO	Subdivided section numbers (not required if NSKO ≤ 0). (NSPNO (I), I=1, NSKO)
CARD 10	1~10	DLZ	Neutron fluxes in reflector by one-dimensional calculation are printed for MNZ positions with interval DLZ cm from the boundary to (DLX×MNZ) cm (not required if MNZ < 0).
CARD 11	1~3	KLB	Lower boundary condition (Z-coordinate).
	4~6	KPT	Upper boundary condition (Z-coordinate).
	7~9	KL	Left boundary condition (X-coordinate).
	10~12	KR	Right boundary condition (X-coordinate).
	13~15	KB	Back boundary condition (Y-coordinate).
	16~18	KT	Front boundary condition (Y-coordinate).

Following four boundary conditions are accepted :

=0 Zero flux.

=1 Zero derivative

=2 Logarithmic derivative ;

$$\frac{d\phi}{dr} = -\frac{\phi}{\gamma}, \gamma \text{ is input (see CARD 12~17).}$$

=3 Analytical ;

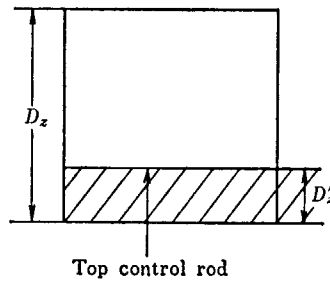
Inside of the boundary the finite difference method is applied and outside of it, the neutron flux is solved analytically. These two methods are combined with the continuity conditions of neutron flux and current at the boundary.

Card number	Column	Variable name	Comments
CARD 12		C1	The value of logarithmic derivative for KLB (used only if KLB=2).
	1~10	C1 (1)	For first group,
	11~20	C1 (2)	For second group,
	21~30	C1 (3)	For third group.
CARD 13	(3E10.0)	C2	The value of logarithmic derivative for KPT (used only if KPT=2). (C2 (NG), NG=1, NGMAX).
CARD 14	(3E10.0)	GAM1	The value of logarithmic derivative for KL (used only if KL=2). (GAM1 (NG), NG=1, NGMAX)
CARD 15	(3E10.0)	GAM2	The value of logarithmic derivative for KR (used only if KR=2). (GAM2 (NG), NG=1, NGMAX)
CARD 16	(3E10.0)	GAM3	The value of logarithmic derivative for KB (used only if KB=2). (GAM3 (NG), NG=1, NGMAX)
CARD 17	(3E10.0)	GAM4	The value of logarithmic derivative for KT (used only if KT=2). (GAM4 (NG), NG=1, NGMAX)
CARD 18	(3E10.0)	YK	Fission spectrum. (YK (NG), NG=1, NGMAX)
CARD 19	1~3	ITIN 1	Maximum number of inner iterations for two-dimensional calculation to obtain initial source guess.
	4~6	IPMAX 1	Maximum number of source iterations in the same routine as above.
	7~9	INITSC	Option of acceleration in the same routine as above. =0 SLOR (Successive Line Over Relaxation) is applied to X- and Y-coordinate. =1 SLOR is applied only to X-coordinate.
CARD 20	1~10	EPSI (1)	Eigenvalue convergence criterion of one-dimensional calculation to obtain initial source guess.
	11~20	EPSI (2)	Source distribution convergence criterion in the same routine as above.
	21~30	EPS 2	Convergence criterion of inner iterations of two-dimensional calculation to obtain initial source guess.
	31~40	EPS 1	Convergence criterion of source iterations in the same routine as above.
CARD 21	1~10	THETA	Acceleration factor for one-dimensional calculation.
	11~20	W	Acceleration factor for source iterations is two-dimensional calculation.
CARD 22	1~3	IP3MAX	Maximum number of source iterations in three-dimensional calculation.
	4~6	ITMAX	Maximum number of inner iterations in three-dimensional calculation.

Card number	Column	Variable name	Comments
CARD 22	7~9	ITR 1	Number of inner iterations to exchange the convergence criteria for three-dimensional calculation. ITR 1 and ITR 2 have correlation with following EPI (1) and EPI (2).
	10~12	ITR 2	
CARD 23	1~10	CRT 2	Convergence criterion of source iterations in three-dimensional calculation.
	11~20	EPI (1)	Initial convergence criterion for inner iterations in the same routine as above (used for source iteration number < ITR1).
	21~30	EPI (2)	Intermediate convergence criterion for inner iterations in the same routine as above (used for source iteration number < ITR2).
	31~40	EPI (3)	Final convergence criterion for inner iterations in the same routine as above.
CARD 24	1~10	WXY	Acceleration factor for L_{xy}
	11~29	WZS	Acceleration factor for L_z
	21~30	WS	Acceleration factor for source iterations.
CARD 25			Required only if IGS=1.
	1~3	NAMAX	Number of sections in Z-coordinate
	4~6	IIMAX	Number of mesh points in X-coordinate
	7~9	JJMAX	Number of mesh points in Y-coordinate
CARD 26			Initial source guess for one-dimensional calculation (required only if IGS=1). (A (N), N=1, MAMAX)
			CARD 26 is repeated NMAX times.
CARD 27			Initial source guess for two-dimensional calculation (required only if IGS=1). (A (N), N=1, KKKMAX), where KKKMAX=IIMAX*JJMAX.
			CARD 27 is repeated KMAX times.
CARD 28			Number of types of blocks with different diffusion parameters (required only if KKK=4).
CARD 29			Diffusion parameter
	1~10	D	Diffusion coefficient in core, D
	11~20	STR	Removal cross-section in core, Σ_r
	21~30	SSA	Absorption cross-section in core, Σ_a
	31~40	SVU	Emission cross-section in core, $\nu\Sigma_f$
	41~50	ALXY	Initial guess of radial leakage, L_{xy}
	51~60	AKSF	Power per fission
	61~70	ANU	Number of emitted neutron per fission, ν
			CARD 29 is repeated as follows.
		KKK=1	NGMAX times.
		KKK=2	NMAX groups are required, one of which consists of NGMAX cards.
		KKK=3	KMAX groups are required, one of which consists of

Card number	Column	Variable name	Comments
			NGMAX cards and they are required NMAX times.
		KKK=4	NGMAX cards are repeated by number of fuel types.
CARD 30			Required only if ILXY=1.
	1~3	NK	Number of channels for which initial guess of radial leakage is input.
	4~6	KK	Number of blocks of the channel.
	7~9	NGK	Number of energy groups.
CARD 31			Initial guess values of radial leakage (required only if ILXY=1).
			(ALXY (N, K, G), G=1, NGK)
			CARD 31 is repeated KK*NK times.
CARD 32	1~10	DB	Diffusion coefficient of lower reflector.
	11~20	STRB	Removal cross-section of lower reflector.
	21~30	SSAB	Absorption cross-section of lower reflector.
	31~40	BUKB	Geometrical buckling of lower reflector.
			CARD 32 is repeated NGMAX times.
CARD 33	1~10	DT	Diffusion coefficient of upper reflector.
	11~20	STRT	Removal cross-section of upper reflector.
	21~30	SSAT	Absorption cross section of upper reflector.
	31~40	BUKT	Geometrical buckling of upper reflector.
			CARD 33 is repeated NGMAX times.
CARD 34	1~10	DR	Diffusion coefficient of right side reflector.
	11~20	STRR	Removal cross-section of right side reflector.
	21~30	SSAR	Absorption cross section of right side reflector.
	31~40	BUKR	Geometrical buckling of right side reflector.
			CARD 34 is repeated NGMAX times.
CARD 35			If NCROD<0, not required
	1~10	GBASE	Values of logarithmic derivative at the surface of control-rod.
	11~20	GDD	Diffusion coefficient of control-rod.
	21~30	GSR	Removal cross-section of control-rod.
	31~40	GSA	Absorption cross-section of control-rod.
	41~50	GCR	Initial guess value of radial leakage L_{CR} of control-rod.
			CARD 35 is repeated NGMAX times.
CARD 36			If NCROD<0, not required
	1~10	WHT	Weighting factor to correct the logarithmic derivative value in a block which contains the top of a control-rod.
			Logarithmic derivative value γ is corrected to γ' in the following manner:
			$-\gamma' = -\gamma \cdot \frac{DZ}{DZ'} \cdot WHT$

Card number	Column	Variable name	Comments
-------------	--------	---------------	----------



CARD 37

Blank card.

4.4 Output description

Following data are printed but the items marked with * are the optional output.

- 1 Input data
- 2* Eigenvalue of two-dimensional diffusion equation integrated over Z axis for obtaining the initial source guess.
- 3 Eigenvalue of three-dimensional diffusion equation.
- 4 Averaged neutron source, power, neutron flux and neutron leakage in each block.
- 5 Neutron flux and source distribution along Z axis in each channel.
- 6* Neutron flux distribution in the reflector.
- 7 Two-dimensional neutron flux distribution in each layer.
- 8* Thermal neutron flux at the positions of in-core monitors.

Either of the following data is punched out.

- 1 Neutron source at each mesh point. The punched data are channel-wise neutron sources for one-dimensional calculation and layer-wise neutron sources for two-dimensional calculation. The numbers of mesh points along Z axis, X and Y axes are punched on the first card with the format (3I3). The neutron sources are punched in the format (7E10.3).
- 2 Radial leakage L_{xy} in each block. The first card contains numbers of channels, blocks and energy-groups in the format (3I3). The values of L_{xy} are punched in the format (7E10.3).

4.5 Sample problem

The geometry of the sample problem is a quarter core of JPDR-II whose X-Y cross section is shown in Fig. 13. A channel is divided into four meshes. Left and back side reflectors have one mesh point at each X and Y coordinate. In the outside of the mesh point, neutron flux is calculated analytically. A channel is divided into sections along Z axis as shown in Fig. 14 and the top and bottom boundary conditions are both "analytical". The blocks from 1 to 8 of the No. 1, 2 and 3 channels contain heavy absorber.

The input and output data of this problem are shown in Appendix A and B, respectively. The computation time and core memory required for this computation on the FACOM 230-75 are as follow :

CPU time	346sec,
Core time	884sec,
Core memory	105K words.

5. Conclusions

The new "leakage iterative method", embodied in the DIFFUSION-ACE code for the FACOM 230-75 and COC-6600 computers, has been shown to make it possible to analyse a reactor core performance by the finite difference approximation with much less mesh points and shorter computer time than by the conventional fine mesh finite difference method. The discretization error is small in comparison with the coarse mesh method in the calculation of neutron leakage from a subregion.

A good agreement has been obtained between the computed results by the DIFFUSION-ACE and those by the ADC based on the conventional fine mesh difference approximation method. It has been confirmed that the iteration scheme employed in DIFFUSION-ACE converge smoothly.

Acknowledgments

The authors wish to express their appreciation to M. Akimoto for his guide for using the computer code ADC written by him. Thanks are also rendered to T. Asaoka and S. Matsuura of the Japan Atomic Energy Research Institute for their valuable discussions.

References

- 1) WACHSPRESS, E. L., BURGESS, E. L. and BARON, S.: *Nucl. Sci. Eng.*, **12**, 381 (1962).
- 2) HENRY, A. F.: "Refinements in Accuracy of Coarse Mesh Finite Difference Solution of the Reactor Calculation", IAEA/SM-154/21, International Atomic Energy Agency, Vienna (1972).
- 3) VARGA, R. S.: "Matrix Iterative Analysis", Academic Press, New York (1971).
- 4) PEACEMAN, D. W. and RACHFORD, H. H.: *J. Soc. Indust. Appl. Math.*, **3**, 28 (1955).
- 5) AKIMOTO, M. and NAITO, Y.: "A General Dimensional Neutron Diffusion Calculation Code: ADC", JAERI 1260 (1979).

APPENDIX A Sample Input

CONTROL DATA 3600 DATA INPUT FORM

[illegible]

DATA DESCRIPTION*

PREPARED BY

DATE _____ PAGE 1 OF _____


Century Research Center Corporation

CONTROL DATA 3600 DATA INPUT FORM

	1	2	3	4	5	6	7	8	9	10	11	12	13	14	15	16	17	18	19	20	21	22	23	24	25	26	27	28	29	30
01	3	3	3	3	3	3	3	3	3	3	3	3	3	3	3	3	3	3	3	3	3	3	3	3	3	3	3	3	3	3
02	4	4	4	4	4	4	4	4	4	4	4	4	4	4	4	4	4	4	4	4	4	4	4	4	4	4	4	4	4	4
03	4	4	4	4	4	4	4	4	4	4	4	4	4	4	4	4	4	4	4	4	4	4	4	4	4	4	4	4	4	4
04	1	4	3	5	1	1	4	9	5	3	2	E-1	1	1	1	1	1	1	1	1	1	1	1	1	1	1	1	1	1	1
05	0	6	9	8	8	1	1	7	9	8	1	E-1	1	1	1	1	1	1	1	1	1	1	1	1	1	1	1	1	1	1
06	0	2	8	2	0	5	1	0	0	1	1	1	1	1	1	1	1	1	1	1	1	1	1	1	1	1	1	1	1	1
07	1	4	7	2	5	1	1	5	0	7	0	2	E-1	1	1	1	1	1	1	1	1	1	1	1	1	1	1	1	1	1
08	0	6	6	9	2	6	1	8	5	5	1	5	E-1	1	1	1	1	1	1	1	1	1	1	1	1	1	1	1	1	1
09	0	2	8	5	3	4	1	0	0	1	1	1	1	1	1	1	1	1	1	1	1	1	1	1	1	1	1	1	1	1
10	1	4	8	0	1	0	1	5	1	2	9	0	E-1	1	1	1	1	1	1	1	1	1	1	1	1	1	1	1	1	1
11	0	6	7	0	7	1	1	8	7	1	5	7	E-1	1	1	1	1	1	1	1	1	1	1	1	1	1	1	1	1	1
12	0	6	2	8	0	1	4	0	0	1	1	1	1	1	1	1	1	1	1	1	1	1	1	1	1	1	1	1	1	1
13	1	4	8	7	8	1	1	5	1	8	7	7	E-1	1	1	1	1	1	1	1	1	1	1	1	1	1	1	1	1	1
14	0	6	7	2	2	1	1	8	8	7	9	8	E-1	1	1	1	1	1	1	1	1	1	1	1	1	1	1	1	1	1
15	0	6	2	7	4	9	4	0	0	1	1	1	1	1	1	1	1	1	1	1	1	1	1	1	1	1	1	1	1	1
16	1	6	9	8	2	5	1	7	2	5	0	2	E-1	1	1	1	1	1	1	1	1	1	1	1	1	1	1	1	1	1
17	0	6	5	8	9	3	1	7	1	5	1	5	8	E-0	1	1	1	1	1	1	1	1	1	1	1	1	1	1	1	1
18	0	6	1	5	9	0	7	0	0	1	1	1	1	1	1	1	1	1	1	1	1	1	1	1	1	1	1	1	1	1
19	1	6	9	8	2	5	1	7	2	5	0	2	E-1	1	1	1	1	1	1	1	1	1	1	1	1	1	1	1	1	1
20	0	6	5	8	9	3	1	7	1	5	1	5	8	E-0	1	1	1	1	1	1	1	1	1	1	1	1	1	1	1	1
21	0	6	1	5	9	0	7	0	0	1	1	1	1	1	1	1	1	1	1	1	1	1	1	1	1	1	1	1	1	1
22	1	6	9	8	2	5	1	7	2	5	0	2	E-1	1	1	1	1	1	1	1	1	1	1	1	1	1	1	1	1	1
23	0	6	5	8	9	3	1	7	1	5	1	5	8	E-0	1	1	1	1	1	1	1	1	1	1	1	1	1	1	1	1
24	0	6	1	5	9	0	7	0	0	1	1	1	1	1	1	1	1	1	1	1	1	1	1	1	1	1	1	1	1	1
25	1	6	9	8	2	5	1	7	2	5	0	2	E-1	1	1	1	1	1	1	1	1	1	1	1	1	1	1	1	1	1
26	0	6	5	8	9	3	1	7	1	5	1	5	8	E-0	1	1	1	1	1	1	1	1	1	1	1	1	1	1	1	1
27	0	6	1	5	9	0	7	0	0	1	1	1	1	1	1	1	1	1	1	1	1	1	1	1	1	1	1	1	1	1
28	1	6	9	8	2	5	1	7	2	5	0	2	E-1	1	1	1	1	1	1	1	1	1	1	1	1	1	1	1	1	1
29	0	6	5	8	9	3	1	7	1	5	1	5	8	E-0	1	1	1	1	1	1	1	1	1	1	1	1	1	1	1	1
30	0	6	1	5	9	0	7	0	0	1	1	1	1	1	1	1	1	1	1	1	1	1	1	1	1	1	1	1	1	1

DATA DESCRIPTION

PREPARED BY

 Century Research Center Corporation

DATE

PAGE 2 OF

APPENDIX B Sample Output

DIFFUSION ACE **** THREE DIMENSIONAL DIFFUSION EQUATION CODE

PROBLEM NO. 1

SAMPLE PROBLEM OF DIFFUSION ACE **** JPD-2 (1/4) CORE

*** CHECK OF THE VARIABLE DIMENSION ***

*** YOUR CALCULATIONAL SYSTEM IS PROPER ***

NO. OF (A) IS UNDER THE LIMIT BY 16826 WORDS

*** YOUR CALCULATIONAL SYSTEM IS PROPER ***

NO. OF (NA) IS UNDER THE LIMIT BY 4852 WORDS

**** CALCULATION SYSTEM ****

NO. OF CHANNELS IN X-DIRECTION	5	NO. OF DIVISIONS IN ONE CHANNEL (X) ..	2
NO. OF CHANNELS IN Y-DIRECTION	5	NO. OF DIVISIONS IN ONE CHANNEL (Y) ..	2
NO. OF BLOCKS IN Z-DIRECTION	10	NO. OF DIVISIONS IN ONE BLOCK (Z)	3
NO. OF CHANNELS IN X-Y PLANE	11		
NO. OF DIVISIONS IN THE REFLECTOR (X-Y)	1		
NO. OF DIVISIONS IN THE REFLECTOR (Z)	0		
NO. OF CONTROL RODS	0		
NO. OF IN-CORE MONITORS	3		
NO. OF SPECIAL BLOCKS DIVIDED THINNER	0		

**** GEOMETRY ****

WIDTH OF ONE CHANNEL IN X-DIRECTION	13.6600 CM
WIDTH OF ONE CHANNEL IN Y-DIRECTION	13.6600 CM
LENGTH OF ONE BLOCK IN Z-DIRECTION	14.6700 CM
WIDTH OF THE REFLECTOR (X-Y)	1.0000 CM
THICKNESS OF THE CONTROL RODS	0.0 CM
LENGTH OF THE REFLECTOR (Z)	0.0 CM

CHANNELS POSITION IN X-Y PLANE

	BACK	
LEFT	*****	RIGHT
*	0 0 0 0 11	*
*	0 10 9 8 7	*
*	0 9 6 5 4	*
*	0 8 5 3 2	*
*	11 7 4 2 1	*

	FORE	

**** CONVERGENCE CRITERIA AND RELAXATION FACTORS ****

CONVERGENCE CRITERIA WHEN CALCULATING SOURCE GUESS

CRITERIA ON EIGENVALUE IN 1-DIM. OUTER IT.	0.001000
CRITERIA ON SOURCE DISTR. IN 1-DIM. OUTER IT.	0.001000
CRITERIA IN 2 - DIMENSIONAL INNER IT.	0.001000
CRITERIA IN 2 - DIMENSIONAL OUTER IT.	0.001000
MAX. ITERATION TIMES IN 2-DIM. INNER IT.	50
MAX. ITERATION TIMES IN 2-DIM. OUTER IT.	50
OVER RELAXATION FACTOR OF 1-DIM. OUTER IT.	0.800000
OVER RELAXATION FACTOR OF 2-DIM. INNER IT.	1.400000
SLOM METHOD IN 2-DIM. INNER IT. IS APPLIED TO ONLY X - AXIS	

CONVERGENCE CRITERIA WHEN CALCULATING 3-DIMENSIONAL SYNTHESIS

TEMPORARY CRITERIA IN 3-DIM. INNER IT. WHEN OUTER IT. TIMES ARE LESS THAN	2	0.010000
TEMPORARY CRITERIA IN 3-DIM. INNER IT. WHEN OUTER IT. TIMES ARE LESS THAN	5	0.002000
FINAL CRITERIA IN 3-DIM. INNER ITERATION	0.001000
CONVERGENCE CRITERIA IN 3-DIM. OUTER ITERATION	0.001000
MAX. ITERATION TIMES IN 3-DIM. INNER IT.	100	
MAX. ITERATION TIMES IN 3-DIM. OUTER IT.	60	
RELAXATION FACTOR OF L-XY IN INNER IT.	0.0	
RELAXATION FACTOR OF L-Z IN INNER IT.	0.0	
RELAXATION FACTOR IN 3-DIM. OUTER IT.	1.400000	

MATERIAL MAP

```

X 0 1 2 3 4 5 6 7 8 9 10 11
Y
0 *****
  *12 12 12 12 12 12 12 12 12 12 12*
1 *
  *12 12 12 12 12 12 12 12 12 12*11 11*
2 *
  *12 12 12 12 12 12 12 12 12*11 11*
3 *****
  *12 12 12*10 10* 9 9* 8 8* 7 7*
4 *
  *12 12 12*10 10* 9 9* 8 8* 7 7*
5 *
  *12 12 12* 9 9* 6 6* 5 5* 4 4*
6 *
  *12 12 12* 9 9* 6 6* 5 5* 4 4*
7 *
  *12 12 12* 8 8* 5 5* 3 3* 2 2*
8 *
  *12 12 12* 8 8* 5 5* 3 3* 2 2*
9 *
  *12*11 11* 7 7* 4 4* 2 2* 1 1*
10 *
  *12*11 11* 7 7* 4 4* 2 2* 1 1*
11 *****

```

**** CONVERGENCE OF 2-DIM. FOR SOURCE GUESS **

SOURCE	IT.	MAX LAMBDA	LAMBDA	MIN LAMBDA	ACC. PARAMETER USED
1		0.12545683E 01	0.11000087E 01	0.79578717E 00	0.0
2		0.11633639E 01	0.11066962E 01	0.92989860E 00	0.0
3		THETA VALUE 0.45172E-01	0.74707E-02	0.88812E-15	0.13177E 28 0.85527E-71
4		0.11467046E 01	0.11110999E 01	0.97417982E 00	0.45172138E-01
5		0.11372903E 01	0.11137898E 01	0.10301718E 01	0.74707407E-02
6		THETA VALUE 0.16240E 01	0.80115E 00	0.24780E 00	0.25102E-01 0.85527E-71
7		0.11269634E 01	0.11177787E 01	0.11030940E 01	0.16239749E 01
8		0.11216661E 01	0.11183248E 01	0.11052834E 01	0.80115178E 00
9		0.11209229E 01	0.11184909E 01	0.11094107E 01	0.24779518E 00
10		0.11207468E 01	0.11185876E 01	0.11116506E 01	0.25102076E-01
11		THETA VALUE 0.11234E 01	0.99834E-01	0.24780E 00	0.25102E-01 0.85527E-71
12		0.11202846E 01	0.11188101E 01	0.11146488E 01	0.11234079E 01
13		0.11204948E 01	0.11188336E 01	0.11158796E 01	0.99834280E-01
14		THETA VALUE 0.18050E 00	0.99834E-01	0.24780E 00	0.25102E-01 0.85527E-71
15		0.11197920E 01	0.11189086E 01	0.11165767E 01	0.18049611E 00
16		THETA VALUE 0.25690E 01	0.14090E 00	0.24780E 00	0.25102E-01 0.85527E-71
17		0.11203633E 01	0.11189529E 01	0.11178572E 01	0.25669607E 01
18		0.11198798E 01	0.11190171E 01	0.11179874E 01	0.14090025E 00

**** SOURCE ITERATION OF 3-DIMENSIONAL DIFFUSION EQUATION ****

IT. TIMES	MAX LAMBDA	LAMBDA	MIN LAMBDA
1	0.38270324E 02	0.11236220E 01	0.67559244E 00
2	0.22431177E 01	0.11072136E 01	0.96035172E 00
3	0.14296138E 01	0.11037212E 01	0.10175050E 01
4	0.12605922E 01	0.11030910E 01	0.10283361E 01
5	0.11900815E 01	0.11023777E 01	0.10367239E 01
6	0.11518746E 01	0.11019269E 01	0.10460768E 01
7	0.11344379E 01	0.11016326E 01	0.10546061E 01
8	0.11262256E 01	0.11013780E 01	0.10617209E 01
9	0.11204805E 01	0.11012571E 01	0.10684738E 01
10	0.11170189E 01	0.11012742E 01	0.10738535E 01
11	0.11131666E 01	0.11012152E 01	0.10787875E 01
12	0.11100534E 01	0.11011447E 01	0.10826100E 01
13	0.11079542E 01	0.11011415E 01	0.10861103E 01
14	0.11065276E 01	0.11011460E 01	0.10889705E 01
15	0.11055497E 01	0.11011579E 01	0.10912995E 01
16	0.11048194E 01	0.11011747E 01	0.10931995E 01
17	0.11040471E 01	0.11012398E 01	0.10942926E 01
18	0.11036367E 01	0.11012098E 01	0.10961447E 01
19	0.11035361E 01	0.11012532E 01	0.10967345E 01
20	0.11032527E 01	0.11012695E 01	0.10975601E 01
21	0.11029775E 01	0.11012783E 01	0.10983790E 01
22	0.11027327E 01	0.11012936E 01	0.10986362E 01
23	0.11025341E 01	0.11013076E 01	0.10988689E 01
24	0.11023782E 01	0.11013215E 01	0.10990710E 01
25	0.11022611E 01	0.11013351E 01	0.10992462E 01
26	0.11021705E 01	0.11013488E 01	0.10994060E 01
27	0.11020862E 01	0.11013618E 01	0.10995618E 01
28	0.11019977E 01	0.11013726E 01	0.10997172E 01
29	0.11019292E 01	0.11013822E 01	0.10998643E 01
30	0.11018772E 01	0.11013910E 01	0.10999917E 01
31	0.11018475E 01	0.11014007E 01	0.11000963E 01
32	0.11018294E 01	0.11014108E 01	0.11001901E 01
33	0.11018319E 01	0.11014188E 01	0.11002887E 01
34	0.11017533E 01	0.11014278E 01	0.11003947E 01
35	0.11017958E 01	0.11014331E 01	0.11004696E 01
36	0.11017376E 01	0.11014388E 01	0.11005538E 01
37	0.11017590E 01	0.11014450E 01	0.11006139E 01
38	0.11019074E 01	0.11014511E 01	0.11006570E 01
39	0.11017491E 01	0.11014553E 01	0.11007366E 01

OUTER ITERATION END

FLUX AND SOURCE DISTRIBUTION

EIGEN VALUE

1.1014553

CHANNEL NO.	1			
BLOCK NO.	SOURCE	FLUX-1G	FLUX-2G	FLUX-3G
1	0.11611E 00	0.24020E 01	0.10745E 01	0.84763E 00
2	0.22463E 00	0.48869E 01	0.21895E 01	0.16245E 01
3	0.32761E 00	0.71266E 01	0.31932E 01	0.23691E 01
4	0.41557E 00	0.90405E 01	0.40510E 01	0.30049E 01
5	0.48684E 00	0.10590E 02	0.47453E 01	0.35201E 01
6	0.54493E 00	0.11820E 02	0.53103E 01	0.39402E 01
7	0.61293E 00	0.13329E 02	0.59732E 01	0.44317E 01
8	0.80847E 00	0.17269E 02	0.77643E 01	0.58630E 01
9	0.13731E 01	0.23933E 02	0.11583E 02	0.12066E 02
10	0.10415E 01	0.17049E 02	0.82426E 01	0.92341E 01

CHANNEL NO.	2			
BLOCK NO.	SOURCE	FLUX-1G	FLUX-2G	FLUX-3G
1	0.17929E 00	0.34693E 01	0.15715E 01	0.13222E 01
2	0.34659E 00	0.70379E 01	0.31948E 01	0.25347E 01
3	0.50512E 00	0.10256E 02	0.46560E 01	0.36938E 01
4	0.64032E 00	0.13002E 02	0.59025E 01	0.46820E 01
5	0.74825E 00	0.15193E 02	0.68972E 01	0.54708E 01
6	0.82963E 00	0.16847E 02	0.76481E 01	0.60654E 01
7	0.89990E 00	0.18297E 02	0.83051E 01	0.65777E 01
8	0.10498E 01	0.21176E 02	0.96265E 01	0.76828E 01
9	0.14542E 01	0.25305E 02	0.12252E 02	0.12780E 02
10	0.10382E 01	0.17009E 02	0.82216E 01	0.92044E 01

CHANNEL NO.	3			
BLOCK NO.	SOURCE	FLUX-1G	FLUX-2G	FLUX-3G
1	0.22744E 00	0.42135E 01	0.19251E 01	0.16879E 01
2	0.43984E 00	0.85392E 01	0.39115E 01	0.32386E 01
3	0.64090E 00	0.12441E 02	0.56992E 01	0.47187E 01
4	0.81228E 00	0.15768E 02	0.72234E 01	0.59799E 01
5	0.94816E 00	0.18406E 02	0.84314E 01	0.69797E 01
6	0.10468E 01	0.20322E 02	0.93093E 01	0.77050E 01
7	0.11158E 01	0.21688E 02	0.99332E 01	0.82112E 01
8	0.12213E 01	0.23629E 02	0.10832E 02	0.89937E 01
9	0.14786E 01	0.25693E 02	0.12444E 02	0.12996E 02
10	0.10106E 01	0.16559E 02	0.80058E 01	0.89584E 01

LEAKAGE DISTRIBUTION

CHANNEL NO. 1							
BLOCK NO.	LZ-1G	LZ-2G	LZ-3G	LXY-1G	LXY-2G	LXY-3G	POWER
1	0.27499E-02	0.34290E-03	-0.64895E-02	-0.71404E-02	-0.32873E-02	-0.12409E-02	0.11601E 00
2	0.32894E-03	0.16127E-03	0.66021E-04	-0.71012E-02	-0.32847E-02	-0.13940E-02	0.22437E 00
3	0.30885E-03	0.15054E-03	0.61488E-04	-0.70550E-02	-0.32826E-02	-0.13877E-02	0.32721E 00
4	0.27680E-03	0.13547E-03	0.53883E-04	-0.70650E-02	-0.32720E-02	-0.13598E-02	0.41504E 00
5	0.20859E-03	0.10038E-03	0.39845E-04	-0.70018E-02	-0.32337E-02	-0.13519E-02	0.48620E 00
6	-0.46417E-05	-0.16512E-05	0.23097E-06	-0.67797E-02	-0.31438E-02	-0.13366E-02	0.54419E 00
7	-0.92807E-03	-0.45251E-03	-0.17846E-03	-0.58598E-02	-0.26969E-02	-0.11497E-02	0.61208E 00
8	-0.25292E-02	-0.20310E-02	-0.27375E-02	-0.34299E-02	-0.14757E-02	-0.46952E-03	0.80783E 00
9	0.48681E-02	0.27483E-02	0.18654E-02	-0.11632E-02	-0.53947E-03	-0.24519E-03	0.13727E 01
10	0.75990E-02	0.24064E-02	-0.41234E-02	-0.18071E-03	-0.81446E-04	-0.20626E-04	0.10414E 01

CHANNEL NO. 2							
BLOCK NO.	LZ-1G	LZ-2G	LZ-3G	LXY-1G	LXY-2G	LXY-3G	POWER
1	0.28246E-02	0.39696E-03	-0.60277E-02	-0.38695E-02	-0.47223E-02	-0.80170E-02	0.17919E 00
2	0.33071E-03	0.16184E-03	0.70608E-04	-0.38170E-02	-0.47232E-02	-0.83728E-02	0.34631E 00
3	0.30904E-03	0.15055E-03	0.61193E-04	-0.38032E-02	-0.47174E-02	-0.83602E-02	0.50469E 00
4	0.28887E-03	0.14118E-03	0.56610E-04	-0.37971E-02	-0.47123E-02	-0.83399E-02	0.63972E 00
5	0.25029E-03	0.12174E-03	0.49518E-04	-0.37697E-02	-0.46912E-02	-0.83294E-02	0.74751E 00
6	0.13049E-03	0.65059E-04	0.29776E-04	-0.36640E-02	-0.46347E-02	-0.82930E-02	0.82877E 00
7	-0.30241E-03	-0.14068E-03	-0.36743E-04	-0.32987E-02	-0.44090E-02	-0.80936E-02	0.89895E 00
8	-0.13754E-02	-0.12964E-02	-0.18988E-02	-0.18336E-02	-0.34214E-02	-0.69989E-02	0.10487E 01
9	0.41500E-02	0.23834E-02	0.16844E-02	-0.36182E-03	-0.22029E-03	-0.17871E-03	0.14537E 01
10	0.69220E-02	0.21062E-02	-0.41962E-02	0.45320E-03	0.21600E-03	0.10323E-03	0.10381E 01

CHANNEL NO. 3							
BLOCK NO.	LZ-1G	LZ-2G	LZ-3G	LXY-1G	LXY-2G	LXY-3G	POWER
1	0.28534E-02	0.42380E-03	-0.57476E-02	-0.15986E-02	-0.56919E-02	-0.12124E-01	0.22736E 00
2	0.33553E-03	0.16378E-03	0.73522E-04	-0.15610E-02	-0.57047E-02	-0.12579E-01	0.43958E 00
3	0.30793E-03	0.15008E-03	0.60818E-04	-0.15383E-02	-0.56962E-02	-0.12366E-01	0.64049E 00
4	0.29506E-03	0.14415E-03	0.57972E-04	-0.15343E-02	-0.56937E-02	-0.12552E-01	0.81170E 00
5	0.26850E-03	0.13072E-03	0.53247E-04	-0.15154E-02	-0.56785E-02	-0.12543E-01	0.94741E 00
6	0.20300E-03	0.10033E-03	0.43502E-04	-0.14628E-02	-0.56472E-02	-0.12514E-01	0.10459E 01
7	-0.92359E-05	0.31684E-05	0.22641E-04	-0.13157E-02	-0.55295E-02	-0.12373E-01	0.11148E 01
8	-0.73777E-03	-0.87787E-03	-0.14221E-02	-0.34798E-03	-0.47498E-02	-0.11350E-01	0.12202E 01
9	0.36283E-02	0.21081E-02	0.15298E-02	0.25369E-03	0.27402E-04	-0.12460E-03	0.14780E 01
10	0.64201E-02	0.18842E-02	-0.42507E-02	0.94452E-03	0.43821E-03	0.19631E-03	0.10105E 01

Z- DIRECTIONAL FLUX DISTRIBUTION

**** CHANNEL NO. 1 ****

	POSITION	SOURCE	1G-FLUX	2G-FLUX	3G-FLUX
1	2.445000	0.8652767E-01	0.1532233E 01	0.6837730E 00	0.6478899E 00
2	7.335000	0.1120135E 00	0.2413148E 01	0.1079111E 01	0.8117676E 00
3	12.225000	0.1497923E 00	0.3260744E 01	0.1460536E 01	0.1083247E 01
4	17.115000	0.1879609E 00	0.4089521E 01	0.1832216E 01	0.1359341E 01
5	22.005000	0.2250404E 00	0.4895888E 01	0.2193567E 01	0.1627488E 01
6	26.895000	0.2608786E 00	0.5675348E 01	0.2542841E 01	0.1886638E 01
7	31.785000	0.2952905E 00	0.6423731E 01	0.2878276E 01	0.2135455E 01
8	36.675000	0.3281737E 00	0.7138823E 01	0.3198731E 01	0.2373210E 01
9	41.565001	0.3593630E 00	0.7817121E 01	0.3502704E 01	0.2598702E 01
10	46.455001	0.3886651E 00	0.8455427E 01	0.3788797E 01	0.2810468E 01
11	51.345001	0.4162057E 00	0.9054391E 01	0.4057228E 01	0.3009554E 01
12	56.235002	0.4418278E 00	0.9611570E 01	0.4306899E 01	0.3194765E 01
13	61.125002	0.4654258E 00	0.1012473E 02	0.4536664E 01	0.3365350E 01
14	66.015001	0.4873991E 00	0.1060246E 02	0.4750734E 01	0.3524172E 01
15	70.905001	0.5076960E 00	0.1104341E 02	0.4948395E 01	0.3670889E 01
16	75.795000	0.5263433E 00	0.1144610E 02	0.5129267E 01	0.3805801E 01
17	80.684999	0.5449239E 00	0.1184963E 02	0.5310178E 01	0.3940119E 01
18	85.574999	0.5635497E 00	0.1225401E 02	0.5491436E 01	0.4074612E 01
19	90.464998	0.5821640E 00	0.1265945E 02	0.5673207E 01	0.4209292E 01
20	95.354998	0.6009032E 00	0.1326044E 02	0.5942577E 01	0.4409110E 01
21	100.244997	0.6468304E 00	0.1406639E 02	0.6303869E 01	0.4676759E 01
22	105.134996	0.6933834E 00	0.1509047E 02	0.6763085E 01	0.5012592E 01
23	110.024996	0.74832118E 00	0.1696885E 02	0.7610950E 01	0.5666292E 01
24	114.914995	0.9488286E 00	0.1974917E 02	0.8919006E 01	0.6910481E 01
25	119.804995	0.1289547E 01	0.2291611E 02	0.1104286E 02	0.1130272E 02
26	124.694994	0.1424391E 01	0.2464006E 02	0.1194733E 02	0.1252782E 02
27	129.584995	0.1405484E 01	0.2424272E 02	0.1175993E 02	0.1236629E 02
28	134.474995	0.1258539E 01	0.2169221E 02	0.1051749E 02	0.1107502E 02
29	139.364994	0.1030295E 01	0.1754614E 02	0.8484118E 01	0.9084236E 01
30	144.254993	0.8356960E 00	0.1190968E 02	0.5726236E 01	0.7543075E 01

FLUX IN THE LOWER REFLECTOR REGION

POSITION	1G-FLUX	2G-FLUX	3G-FLUX
4.890000	0.3409046E 00	0.1726048E 00	0.1282959E 01
9.780000	0.1219894E 00	0.6185176E-01	0.6170612E 00
14.670000	0.4365271E-01	0.2213938E-01	0.2500740E 00
19.560000	0.1562069E-01	0.7922822E-02	0.9490188E-01
24.450000	0.5589715E-02	0.2835138E-02	0.3496134E-01

FLUX IN THE UPPER REFLECTOR REGION

POSITION	1G-FLUX	2G-FLUX	3G-FLUX
4.890000	0.2676583E 01	0.1508165E 01	0.1138209E 02
9.780000	0.9579530E 00	0.5448628E 00	0.5447696E 01
14.670000	0.3428527E 00	0.1954279E 00	0.2207331E 01
19.560000	0.1227075E 00	0.6997873E-01	0.8379294E 00
24.450000	0.4391719E-01	0.2504837E-01	0.3087815E 00